Restarting the economy while saving lives under Covid-19*

Carlo Favero‡ Andrea Ichino§ Aldo Rustichini¶

June 22, 2020

Abstract

We provide, calibrate and test a realistic model of the spread of SARS-Cov-2 in an economy with different risks related to age and sectors. The model considers hospital congestion and response of individuals adjusting their behavior to the virus' spread. We measure precisely the size of these effects using real data for Italy on intensive care capacity and mobility decisions; thus our claim is that the tradeoffs we estimate are quantitatively, rather than qualitatively, approximately correct.

We characterize the policies of containment of the epidemic that are efficient with respect to number of fatalities and GDP loss. Prudent policies of gradual return to work may save many lives with limited economic costs, as long as they differentiate by age group and risk sector. More careful behavior of individuals induced by the perceived cost of infection may contribute to further reduce fatalities.

JEL-Code: I12, I18, D6, H84

Keywords: Covid-19,SARS-Cov-2 SEIR model, post lockdown policies.

*We thank Luca Badolato and Marco Olivari for superb research assistance. We are grateful to Dario Gregori, of the Department of Cardio Toracic Vascular Science and Public Health at the University of Padua and coordinator of the project COVID-19 Italia, for repeated discussions on hospital saturation prevention policies implemented in Veneto, that have influenced our view of the role of these factors. The idea of extending the SEIR model to endogeneize the ICU constraint emerged in discussions between one of the authors and Yakov Amihud. We are also grateful to Massimo Anelli, Gaetano Basso, Michele Boldrin, Giacomo Calzolari, Francesco Cingano, Rubern Durante, Luigi Guiso, Giacomo Ichino, Francesco Lippi, Andrea Mattozzi, Daniele Terlizzese, Eliana Viviano and Giulio Zanella for insightful discussions. All errors are ours.

‡Bocconi University, IGIER, and CEPR; carlo.favero@unibocconi.it.

§European University Institute, University of Bologna, CEPR, CESifo and IZA; andrea.ichino@eui.eu.

¶University of Minnesota, rusti001@umn.edu .

1 Introduction

The main question all countries are facing throughout the world is how to restart the economy while saving lives once the initial diffusion of Covid-19 has been put under control, thanks to emergency lock down measures. We present a model and simulations answering this question, and apply them to data from two emblematic Italian regions: Lombardia and Veneto. These contiguous areas in the north of the country were the first in Italy to be hit by the Covid-19 outbreak (at about the same time) but experienced very different evolutions of the infection. While in Lombardia, with a population of about 10 ml people, 16557 persons died because of Covid-19 between February 24 and June 20, 2020, in Veneto, with a population of 4.9 ml, the same happened to only 2002 persons.[1] We show that these differences are due to factors likely to operate in every country, and are in fact instances of worst and best case scenarios: thus the model is of general interest.

A simulation of the effects of different strategies in these two regions is instructive for a wider audience because Lombardia and Veneto capture well the dichotomy of Covid-19 experiences that is emerging throughout the world, between areas hit very severely and areas hit more mildly by the pandemic. The main factors determining this dichotomy are differences in population density, delays in reacting correctly during the early phase of the infection, and constraints in the number of intensive care places in hospitals (which is shortened to HC in what follows). The simulations we present are based on a reformulation of the $SEIR$ model (Allen, 2017) specifically designed to capture these factors. The basic compartmental model of diseases divides the population in three compartments with homogeneous characteristics: Susceptible, Infectious, and Recovered or Removed, from which the acronym SIR (Kermack and McKendrick, 1927). The $SEIR$ model extends the standard dynamics as for many important infections there is a significant incubation period in which individuals are Exposed, i.e. infected but not yet infectious. Since this is an essential feature of the current virus infection, using $SEIR$ instead of SIR is important to insure that the estimates are quantitatively and not only qualitatively correct.

A second substantial innovation is motivated by the observation that the lethality of Covid-19 increases with age presenting a clear discontinuity at age fifty. As of June 20, 2020, out of more than 33000 fatalities in Italy, less than 400 were of subjects younger than fifty and less than 25 of subjects younger than 30. Moreover, the degree of proximity between workers operating in different sectors has been shown to affect the risk of contagion for this virus.[2] Therefore, our model allows for a differentiation of the population by sectors

[1] Official data from the Italian "Protezione Civile".

[2] See, for example, Boeri et al. (2020) and Barbieri et al. (2020).

(SEC) and ages (AGE), and thus generalizes the concept of basic reproduction number (R_0) to a matrix. Specifically, our SEIR-HC-SEC-AGE model has two sectors characterized respectively by a low and a high risk of infection, which are calibrated on the basis of the information on workers' proximity contained in Barbieri et al. (2020). As for age, we consider 9 brackets, which are calibrated to match the initial distribution of age in the population of the two regions, and that are characterized by age specific labor force participation rates (taken from national statistics) and by age specific lethality, hospitalization and intensive care (IC) rates due to Covid-19 (taken from Ferguson et al., 2020).[3]

The conclusion that differentiation by age can help in choosing good policies is obvious. If the aim is to reduce the loss of GDP with a minimum loss of lives, then at any given state of the economy allowing a younger person (for whom the virus is less lethal) to return to work is better than allowing an older one. A glance at the lethality table by age will offer all that is needed to support this conclusion. The benefit of differentiation by risk sector is just as obvious. But a flight engineer trying to fly a plane will not find the qualitative statement that weight makes the plane fall and lift makes the plan go up very useful: he will need to know the precise quantitative tradeoff. Similarly, the qualitative statement that allowing younger people to return to work is less costly, or its reformulation in an *as if* model capturing the tradeoff, will leave the policy maker equally clueless on what to do.

Instead, our goal is to contrast the economic and public health effects (GDP loss vs. saved lives over a full year) of possible policies to restart the economy that take into account the differences in age specific and sector specific contagion risks. Starting from one extreme with a policy that sends back to work the entire workforce (which we label as policy ALL), the other policies that we study progressively inactivate (i.e. allow only a minimum of the labor force to be active) workers in the high-risk sector, beginning with those belonging to a higher age bracket, until all age brackets and sectors are inactivated (which is the opposite extreme policy labelled as LOCK).

The GDP loss induced by the interaction between the pandemic and the different policies is assumed to be proportional to the number of days in which the policies are in place and to the corresponding fraction of the workforce that is unproductive. In future research we plan to improve on this measure in various ways, particularly with the goal of capturing more long term economic effects of the pandemic. It is likely, however, that the measure of GDP loss we currently use is a lower bound to the total economic cost of the different policies. The number of Covid-19 fatalities associated to the different strategies is predicted by the

[3]In the Online Appendix we present qualitatively similar results based on the analogous parameters estimated by the US Center for Disease Control (CDC). See Garg (2020).

SEIR-HC-SEC-AGE model.[4]

The trade-off between saved lives and GDP losses that characterizes "age based" and "sector based" strategies is not immediately obvious, and its description is our main contribution. The two extreme policies LOCK and ALL provide useful benchmark against which to evaluate the intermediate ones. We now describe our main results.

Taking the policy LOCK as reference, we see that a sequence of policies of return to work for a large fraction of the labor force are feasible, that have a moderate cost in terms of fatalities, as long as they limit the activity of subjects that face a high risk because of their age or because of the sector in which they operate. While we are well aware that each single death due to the current epidemic is a tragedy, we are also keenly aware that the social, mental, and even health implications of a prolonged inactivity are also tragic. Thus, we consider the exploration of these combinations an intellectual duty.

It is therefore possible, along the efficient frontier, to limit the GDP loss within values that are about *one fifth* of the loss incurred locking down the entire economy as done in Italy between March 8 and May 4, 2020. Further containment is also possible, but it may become *extremely* costly in terms of human lives. Depending on the scenario, the cost associated with an unconstrained return to work may be several orders (approximately four times) larger that what is needed to bring the GDP loss close to the 5-10 per cent mark. In the absence of a behavioural response, there is a clear kink in the set of possible efficient outcomes, at which the health costs become substantially larger, that should be very clear and present in the current discussion. This kink is due, in final analysis, to the very different dynamic and health outcomes according to age. Bringing older workers back to work is very costly.

This cost may be in part reduced by the response of individuals who take into account the risk of infection and adjust their behavior to reduce this risk, independently of the administrative measures. We frame this hypothesis in a precise model, assuming that the news on the number of fatalities, which are widely available and frequently communicated in the media, offer reliable information on the number of infected. We estimate the size of the effects of these behavioral adjustments using data on mobility for different types of activities provided by Google. A first evaluation of the effects of such type of adjustments in behavior has been provided by Brotherhood et al. (2020); we provide a testable model and estimate the effects in real data, as part of a research strategy aimed at assessing the quantitative effects of alternative policies.

Our approximation of the effects of the different policies in the presence of a behavioural response to fatalities hinges on the assumption that such response in the future will follow the same pattern that we have observed in the past. Under this assumption, the quantitative

[4]The code to replicate our simulations and estimates is available from the authors.

effect of behavioral adjustments is substantial, and the effect on the shape of the trade-off, represented by the Pareto frontier, dramatic: the curve changes from sharply convex to flat. Whether the assumption of stability in behavioral response is sound is, in our opinion, far from obvious. Behavioral adjustments occurring at the outbreak of the news might themselves be prone to reduction when the epidemic becomes the new normal.

The policies that make this relatively safe return to work possible are a combination of one that has been considered by many government (return to work taking into account the risk specific to each productive sectors) and another one which instead has been totally (and surprisingly) disregarded by the authorities in all countries (differentiation depending on the age of the worker). We think the debate should consider carefully both, and the public should be aware and able to discuss openly both. Since these conclusions are robust to parameters specification, the relative merits of the policies are the same when they are extended to other areas in the world and thus are of immediate interest for an international policy audience.

This paper is obviously related to the large amount of inspiring research that is currently conducted throughout the world on the Covid-19 pandemic[5] and specifically to the literature that has considered the possibility to differentiate containment policies by age.[6] We differ, however, from this literature because we do not aim at suggesting an optimal policy based on some welfare function. Our goal is to measure as precisely as possible, in a specific geographic context, the policy trade off between economic and public health costs of the strategies to deal with the pandemic, so that politicians and the public opinion can make an informed choice. In this respect, the analysis in Acemoglu et al. (2020) is close to ours, but we make an effort to base our analysis on real data for two specific and emblematic geographic contexts. Even if geographically focused, however, our paper offers a more general message which is valid also for other areas and our code can be applied to other contexts with the appropriate corresponding parameterization and data.

The rest of the paper is organized as follows. In Section 2 we introduce some basic epidemiological concepts, while in Section 3 we model the decision process of agents who can take actions that may affect their probability of getting infected and thus the spread of the virus in the population. Section 4 brings the model to the data and estimates the mobility response of subjects to news about infection, using Google mobility data. In Section 5, we

[5]Without aiming for an exhaustive review of the literature, some of the most relevant related papers are: Atkeson (2020), Berger et al. (2020), Durante et al. (2020), Eichenbaum et al. (2020), Fang et al. (2020), Garibaldi et al. (2020) Glover et al. (2020), Greenstone and Nigam (2020), Hall et al. (2020) and Piguillem and Shi (2020)

[6]For example: Acemoglu et al. (2020), Alvarez et al. (2020), Baqaee et al. (2020), Brotherhood et al. (2020), Farboodi et al. (2020), Garriga et al., Gollier (2020), Jones et al. (2020), Kudlyak et al., and Rampini (2020).

explain how we extend the basic SEIR model to a SEIR-HC-SEC-AGE model. Section 6 describes the calibration of the parameters designed to capture the situation of Lombardia and Veneto and to characterize the different policies. Section 7 presents the results, which are discussed in Section 8 together with an analysis of the limits of our simulations.

2 Basic Epidemiological Concepts

Our goal is to model the decision process of agents in an epidemic who have to make choices (such as shopping or going to work) that may affect the probability of getting infected, thereby contributing to the spread of the epidemic. We also want to take into account the incentives provided by the self-interested trade-off analysis of cost and benefits that drives individual behavior independently of the introduction of administrative restrictions as well as the reactions to these restrictions. Before presenting this model, however, we first need to establish some basic epidemiological concepts and notation.

2.1 SEIR Model

The basic SEIR model (Allen, 2017) is described in Figure 1. Time is measured in days and is denoted by t. An initial total population of N_0 individuals is divided into the first infectious subject ($I_0 = 1$) and $S_0 = N_0 - 1$ susceptible subjects. In each subsequent day t some susceptibles become exposed. The daily quantity of new exposed that become new infectious after an incubation period is determined by the net reproduction number of the infection multiplied by the number of existing infectious. The net reproduction number is time varying and it depends on three components: the basic reproduction number (BRN) of the infection, R_0 (i.e. the number of secondary infections each infectious individual produces at the initial stage of the infection in absence of policies or behavioural responses), the average number of days in which a subject is infectious, T_{inf}, and the fraction of susceptibles to the total population,$\frac{S_{t-1}}{N_{t-1}}$, so in each period we have:

$$NewE_t = \frac{R_t}{T_{\text{inf}}} I_{t-1} \quad ; \quad R_t = R_0 \frac{S_{t-1}}{N_{t-1}}$$

The exposed, after an incubation period of T_{inc} days, become infectious. Therefore the outflow from the susceptibles is the inflow into the exposed in each period and, similarly, the outflow from the exposed is the inflow into the infectious, who fall into two categories: those whose destiny is recovery and those whose destiny is to become a fatality. The allocation to these two groups is controlled, respectively by the two probabilities: $1 - p^{fat}$ and p^{fat}. Those who survive the infection are then removed as recovered, REM_REC_t, after a period

Figure 1: Flowchart of the SEIR model

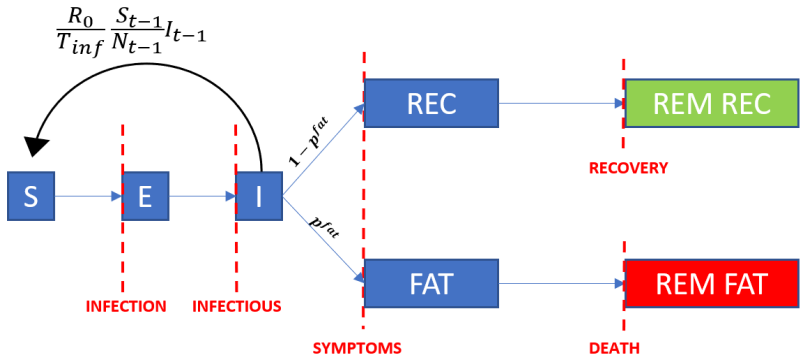

Note: Description of the possible dynamic transitions of a subject in the basic SEIR model (Allen, 2017)

of T_{srec} days from symptoms to recovery. Those who become instead fatalities are removed as fatalities, REM_FAT_t, after a period of T_{sd} days from symptoms to death.

Some comments are necessary to understand the extensions of this basic model that will be presented later. First, a feature of the model is that the lethality of the virus, as measured by

$$\lambda_t^{seir} = \frac{REM\_FAT_t}{E_t + REM\_REC_t + REM\_FAT_t},$$

converges to two possible values only. If $R_0 \leq 1$ the virus diffusion is inhibited and λ_t^{seir} goes to zero. If instead $R_0 > 1$, λ_t^{seir} converges to p^{fat}, which is fixed exogenously. In this second case, the total number of victims will be the same independently of the size of R_0, which determines only the speed at which the asymptotic number of victims is reached. In our extension, the lethalithy of the virus will have instead an endogenous component.

Second, the net reproduction number of the virus varies only as a function of the ratio of the susceptibles to the total population. It is instead reasonable to expect that this variable is affected by policies and by the behavioral response of individuals to the spreading of the virus, two features that will be at the heart of our extension.[7]

Third, all agents within each compartment of the model are identical, while in reality Covid-19 risk is heterogenous across different cohorts of the population and across sectors of activity. This heterogeneity represent another crucial direction in which we extend the basic model

[7] Garibaldi et al. (2020) make this point in the context of matching models and Cochrane (2020) illustrates it in a widely cited blog's post. See also Brotherhood et al. (2020) for another attempt to incorporate behavioural responses in the analysis of the Covid-19 pandemic.

3 Behavioral Response

Several activities (shopping, traveling to work, work, time to consume) are possible at each time unit, say an hour if we want to fix ideas. We are going to examine anyone of these activities, without distinguishing it in the notation.

An appropriate choice of time unit, "short enough", denoted Δt, will allow us to model the matching process in a very simple way, in which a person only meets another person. When we re-scale the process to a time unit of a day, then the number of matches in that longer time unit will be a number

$$M = \frac{1}{\Delta t}. \tag{1}$$

Each individual's value of the activity, indicated by V, is distributed according to a continuous cumulative distribution function F, the same for all consumers. We assume that (i) whether the activity occurs or not does not affect the agent's utility in the next period; (ii) the value process is independent of the health condition of the agent (i.e. on whether he is S, E, I or REM); so the distribution F is health state independent. We omit time subscripts in this section because they are not necessary in this analysis.

People are randomly matched. These are customers who happen to go to the shop at the same time, friends one meets, co-workers, fellow travelers in the subway and so on. We are interested in the matches in which one of the two individuals is I and the other is S. The meeting of an I and an S person result in S-type being infected with probability $\beta(m)$, which is influenced by biological factors and preventive measures (m) taken by the agents (m is mnemonic for masks). We have now to analyze how many individuals an active person meets. Those with a draw of V higher than a threshold v^*, to be determined endogenously, decide to be active (for example, to go out of the house in pursuit of some activity).

Proposition 1 *Let C be the cost of being infected for a subject. The choice of activity is determined by a threshold v^* which solves:*

$$v^* = \frac{I}{N}\beta(m)Pr(V \geq v^*)C. \tag{2}$$

A measure of population density acts as a determinant of the number I of infectious,[8] but we ignore it in the notation for simplicity although it will be relevant in explaining the different effects of the pandemic between the regions that we consider in the empirical analysis (density is almost 60% higher in Lombardia than in Veneto).

[8] Garibaldi et al. (2020) note the similarity of this assumption with the one behind the "matching function" of labor models.

To provide a model for empirical analysis we consider the case in which F is the uniform distribution on $[0, \overline{V}]$, so $F(x) = \frac{x}{\overline{V}}$, for $x \in [0, \overline{V}]$. If we denote the probability of being infected as

$$p \equiv \frac{I}{N}\beta(m) \tag{3}$$

then

$$v^* = \frac{pC}{\overline{V} + pC}\overline{V} \tag{4}$$

so that substituting the value of v^* gives:

$$Pr(V \geq v^*) = \frac{\overline{V}}{\overline{V} + pC} \tag{5}$$

Similar arguments extend to the period after administrative measures (enforced by fines or other penalties) are taken to limit movements (as in lockdown). In this case individuals base their decisions on the expected (taking into account the probability of enforcement) cost of penalties associated for instance with the lockdown, which is independent of the action of others. This is added to the expected cost from becoming infected and therefore also to the right hand side of equation (2), thus increasing the value of v^* which enters into equation (4). If we call K the expected non-negative cost of administrative measures to control the spread of the virus, then one can easily find that:

$$v^* = \overline{V} \min\left\{\frac{pC + K}{pC + \overline{V}}, 1\right\} \tag{6}$$

and therefore:

$$P(V \geq v^*) = \max\left\{\frac{\overline{V} - K}{pC + \overline{V}}, 0\right\}. \tag{7}$$

4 Mobility Data and Behavioral Response

We now provide the link between the simple model presented in the previous section and data on mobility to perform activities in the two Italian regions that we consider. Since time of observation is now crucial we re-introduce the time subscript, but we omit an indicator for the type of activity, which is not necessary for clarity.

Each individual i has to decide whether to perform an activity. She draws utility V_i from a uniform distribution F on $[0, \overline{V}]$. If $V_i \geq v^*_{d,t}$, she becomes active. Note that $v^*_{d,t}$ depends on the day of the week d and on the calendar time t through the policies and the news. Denote as $G_{d,t}$ the total number of activity-driven moves of a given type performed by subjects in a population of size N; we will estimate this value using Google mobility data,

hence the G label. There are of course a variety of types of moves and we rely on three emblematic categories for which Google provides data from various areas around the world and specifically for Lombardia and Veneto during the pandemic:[9] (i) moves to a workplace; (ii) moves to public transport hubs such as subway, bus, and train stations; (iii) moves to grocery markets, food warehouses, farmers markets, specialty food shops, drug stores, and pharmacies.

Google distinguishes between a reference time t_0 corresponding to the five weeks that go from January 3 to February 6, 2020, in which mobility decisions were taken by agents with no Covid-19 concern, and the running time t from February 15 onward in which mobility decisions are taken instead in the presences of concerns about the Covid-19 epidemic. Assuming that the random variables for each individual are independent, the variable underlying the Google measure of mobility, denoted by $G_{d,t}$, is the number of individuals with value V_i larger than $v^*_{d,t}$, and who are therefore active. Note that $G_{d,t}$ depends on d and t through $v^*_{d,t}$. The measure of mobility provided by Google for each type of move is defined by:

$$g_{d,t} = \frac{G_{d,t}}{median(G_{d,t_0})} - 1 \tag{8}$$

which is the relative change in the number of moves of a given type between calendar day t and the same day-of-the-week d during the reference period t_0. Descriptive statistics for these indicators are reported in Table 1.

Table 1: Descriptive statistics for the Google mobility measures

	Mean	Std. Dev.	Min	Max
Lombardia				
Workplace moves	-.47	.24	-.92	.01
Transportation moves	-.62	.26	-.92	.08
Grocery moves	-.31	.24	-.95	.3
Veneto				
Workplace moves	-.40	.23	-.91	.02
Transportation moves	-.56	.28	-.92	.27
Grocery moves	-.27	.28	-.96	.28

Note: the table reports descriptive statistics for the three Google mobility measures that we consider, over the period of 112 days going from February 15, 2020 until the data are available. For each type of move, the measure is the change of the number of moves on a given day relative to the same day-of-the-week in the reference period defined as January, 6 – February, 3, 2020.

The two panels of Figure 2 display, separately for Lombardia and Veneto, the evolution

[9]These data and the related documentation can be found at this link: https://www.google.com/covid19/mobility/.

of fatalities and of the average $g_{d,t}$ for the three types of moves from February 15, 2020, until the data are available. Note that mobility first declined substantially before the Lockdown, on February 23, two days after the first red zone in the city of Codogno was created in Italy and the outbreak of the pandemic became the central news in all the media. Mobility fell again immediately after the Lockdown and started to raise back after fatalities levelled off at the beginning of April. At the end of the observation period mobility has not yet gone back to the levels of the reference period even if fatalities have declined to almost zero.

Since the median of a binomial random variable is equal to one of the two integers defining the interval containing the mean, we can take:

$$\text{median}(G_{d,t_0}) \sim \left((1 - F(v^*_{d,t_0})\right) N$$

where $\sim$ in this case indicates that the difference between the two terms is less than $1/N$; and therefore:

$$g_{d,t} = \frac{v^*_{d,t_0} - v^*_{d,t}}{\overline{V} - v^*_{d,t_0}}$$

which gives the Google measure of mobility $g_{d,t}$ as a linear function of $v^*_{d,t}$, respectively for each type of move. Remember from Section 3 that

$$v^* = \overline{V} \min\left\{\frac{pC + K}{pC + \overline{V}}, 1\right\} = \overline{V}\frac{pC + K}{pC + \overline{V}} \tag{9}$$

where the second equality follows if we make the reasonable assumption that K is smaller than $\overline{V}$ (and in fact we never observe a complete lack of movement). Therefore $g_{d,t}$ can be written as:

$$g_{d,t} = \frac{v^*_{d,t_0}}{\overline{V} - v^*_{j,d,t_0} - \frac{\overline{V}}{\overline{V} - v^*_{d,t_0}}} \frac{pC + K_t}{pC + \overline{V}}$$

Using equation (3), and defining $\tilde{p} \equiv \frac{\beta(m)}{N}$, $g_{d,t}$ is a simple function of the parameters, non-linear in the number of infectious I_t:

$$g_{d,t} = \frac{v^*_{d,t_0}}{\overline{V} - v^*_{d,t_0}} - \frac{\overline{V}}{\overline{V} - v^*_{d,t_0}} \frac{I_t + \frac{K_t}{C\tilde{p}}}{I_t + \frac{\overline{V}}{C\tilde{p}}} \tag{10}$$

More precisely, equation (10) defines a convex function of I_t, with finite derivative at 0, tending to an asymptotic value of - 1 as the number of infectious becomes large. The curve is shifted down when the value of K_t is larger.

It is well known that during the pandemic precise information on the number of infectious was not available in Italy (as well as elsewhere) for two reasons. First, testing was not

Figure 2: Evolution of mobility during the pandemic

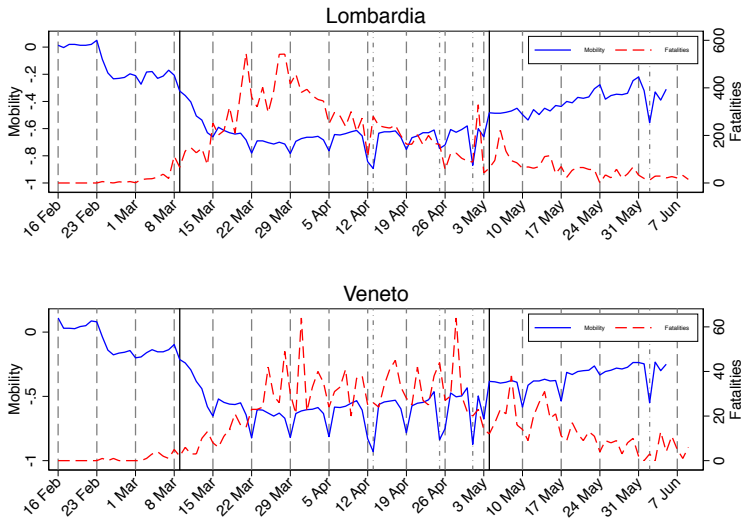

Note: The figure displays the daily average of the Google mobility measure for workplaces, transit and grocery. For each type of mobility, the measure is the change of the number of moves on as given day relative to the same day-of-the-week in the reference period defined as January, 6 – February, 3, 2020. Grey dashed vertical bars denote sundays. The two black solid bars denote, respectively, the beginning of the Lockdown on March 8, 2020 and the beginning of the Phase 2 on May 4.

conducted massively and randomly. Second, asymptomatic infectious subjects could not be detected immediately after contagion, even with massive and random testing. Fatalities due to Covid-19 have instead been measured more precisely during the pandemic and were announced by the media on a daily basis with great emphasis. To estimate equation (10) we therefore assume that during the pandemic subjects were taking the daily number of fatalities as an indirect proxy of the number of infectious I_t.[10]

Table 2 reports non-linear least square estimates of equation (10) for the three mobility indicators and for their average in the last column. As expected, given how the measures are constructed, the first row of the Table shows that the term $\frac{v^*_{d,t_0}}{\overline{V}-v^*_{d,t_0}}$ is estimated to be small and not distinguishable from 0 in the case of grocery. This finding derives from the fact that the probability of moving in a unit of time was on average relatively higher in the reference period before the pandemic particularly for the case of more necessary moves like those for grocery. Consistently with these estimates, the term $-\frac{\overline{V}}{\overline{V}-v^*_{d,t_0}}$ is found to approach -1 and becomes indistinguishable from -1 in the case of Grocery (second row).

The third and fourth rows report estimates of $\frac{K_t}{C\tilde{p}}$, a quantity that is proportional to the severity of the restrictions imposed by the government during the Lockdown and the Phase

[10] A drawback of this assumption is that fatalities in a given day reflect the number of infectious 15-20 days before. In the Online Appendix we present results based on the number of new infectious that was announced daily by health authorities. Results are qualitatively similar.

2 respectively.

Table 2: Non-linear least square estimates of behavioural responses

	Workplace	Transport	Grocery	Average
$\frac{v^*_{d,t_0}}{\overline{V}-v^*_{d,t_0}}$	-0.08***	-0.11***	0.02	-0.06***
	(0.01)	(0.02)	(0.02)	(0.02)
$-\frac{\overline{V}}{\overline{V}-v^*_{d,t_0}}$	-0.74***	-0.76***	-0.95***	-0.70***
	(0.05)	(0.03)	(0.22)	(0.04)
$\frac{K_t}{C\tilde{p}} \approx$ Lockdown	94.61***	14.90***	163.26***	41.66***
	(24.66)	(3.99)	(57.28)	(11.46)
$\frac{K_t}{C\tilde{p}} \approx$ Phase2	42.77***	5.76**	114.47***	20.24***
	(13.42)	(2.33)	(42.09)	(6.74)
$\frac{\overline{V}}{C\tilde{p}}$	163.21***	22.56***	540.80**	73.49***
	(46.94)	(5.31)	(267.80)	(19.44)
$\Delta\overline{V}$ for Lombardia	16.12*	15.81***	83.01	23.03***
	(9.72)	(4.19)	(53.82)	(7.68)
$\Delta\frac{\overline{V}}{C\tilde{p}}$ for Sundays	60.10***	-1.02	-338.83**	-18.70***
	(20.52)	(2.16)	(158.82)	(5.40)
$\Delta\frac{\overline{V}}{C\tilde{p}}$ for Easter	-85.00***	-9.60**	-68.70*	-28.83***
	(23.33)	(3.96)	(39.20)	(8.00)
$\Delta\frac{\overline{V}}{C\tilde{p}}$ for April 25	-45.99**	-5.65	-375.47**	-40.80***
	(23.30)	(8.79)	(173.61)	(11.76)
$\Delta\frac{\overline{V}}{C\tilde{p}}$ for May 1	-80.48***	-7.01	-384.31**	-42.97***
	(22.75)	(5.21)	(182.86)	(10.62)
$\Delta\frac{\overline{V}}{C\tilde{p}}$ for June 2	-121.04***	-6.17	-313.82**	-45.91***
	(32.48)	(6.04)	(157.69)	(11.58)
Observations	224	224	224	224
Adj R-squared	0.85	0.83	0.73	0.83

Note: the table reports non-linear least square estimates of equation (10), using daily information on Google mobility measures and official figures on fatalities for Lombardia and Veneto from February 15, 2020 until June 5, 2020. For each type of mobility, the measure is the change of the number of moves on a given day relative to the same day-of-the-week in the reference period defined as January, 6 – February, 3, 2020. Lockdown and Phase2 are, respectively, dummies for the period between March 8 and May 3, 2020 and the period between May 4 and June1 5, 2020. April 25, May 1 and June 2 celebrate, respectively, the end of WW2, the labor day and the beginning of the Italian Republic.

The estimates suggest that restrictions were lifted by about a half on average during Phase 2 with respect to the Lockdown (last column). The lifting of restriction was actually more intense for transport than for grocery, a type of move for which regulations did not change too much between the two phases.

In the fifth row, in line with the assumptions of our model, $\frac{\overline{V}}{C\tilde{p}}$ is estimated to be higher than $\frac{K_t}{C\tilde{p}}$ for both the Lockdown and Phase2. The ranking of these three estimates for each type of move is a central result of this estimation exercise and captures the effect of the

policies with respect to normal times. This result is better shown in Figure 3 which is based on the estimates in the last column of Table 2 for the average of the three mobility measures. The figure displays the scatter plot of daily fatalities and average mobility. The different markers of the scatter plot identify the three periods for which we have data: Pre-lockdown, Lockdown and Phase 2. The figure also plots predictions from locally weighted regressions as well as predictions based on the estimates in column 4 of Table 2.

Within each of the three phases we cannot reject that the relationship between mobility and daily fatalities is negative and convex as predicted by the model.

This negative and convex relationship within each phase is the behavioural response of subjects to the variation of the contagion risk, in the absence of policies.[11]

The parallel downward shift between the circles and the squares is the effect of the Lockdown, which has reduced mobility for any level of fatalities. The upward shift from the squares to the triangles is instead the effect of the softening of restrictions during the Phase 2 with respect to the Lockdown. While it is evident that policies were effective, this Figure clearly shows that Cochrane (2020) hypothesis of an endogenous response to the number of infectious cannot be dismissed and it is quantitatively important. Of course, the short time horizon on which these estimates are computed does not guarantee that in the long run this behavioural effect would maintain the same intensity, as individuals may become used to the presence of Covid-19 and less responsive to news related to the effects of the disease.

Coming back to Table 2, the remaining rows of the table show estimates of how $\frac{\overline{V}}{C\overline{p}}$ changes in Lombardia with respect to Veneto and on holidays with respect to working days. Coeteris paribus, the utility of moving is higher in Lombardia, leading to a slightly smaller reduction of mobility in this region with respect to the reference period, particularly in the case of transports. As for holidays, as expected given Figure 2, they all tend to reduce mobility of the kind considered here.

5 SEIR-HC-SEC-AGE Model

Building on the analysis conducted so far, our objective is to provide a realistic empirical model with two main features. First, the capability of replicating the dynamics of the virus observed in two emblematic benchmark cases (Lombardia and Veneto) before and during the lockdown. Second, the ability to simulate outcomes of different policies of containment

[11] Cochrane (2020) states clearly that, as a consequence of the omission of this response, "the SIR model has been completely and totally wrong". Durante et al. (2020) also find that after the virus outbreak mobility declined in Italy, but significantly more in areas with higher civic capital, both before and after a mandatory national lockdown. Civic capital is however likely to be irrelevant for our analysis since all available measures suggest the absence of significant differences in this variable between Lombardia and Veneto.

Figure 3: Behavioural responses to news and policies

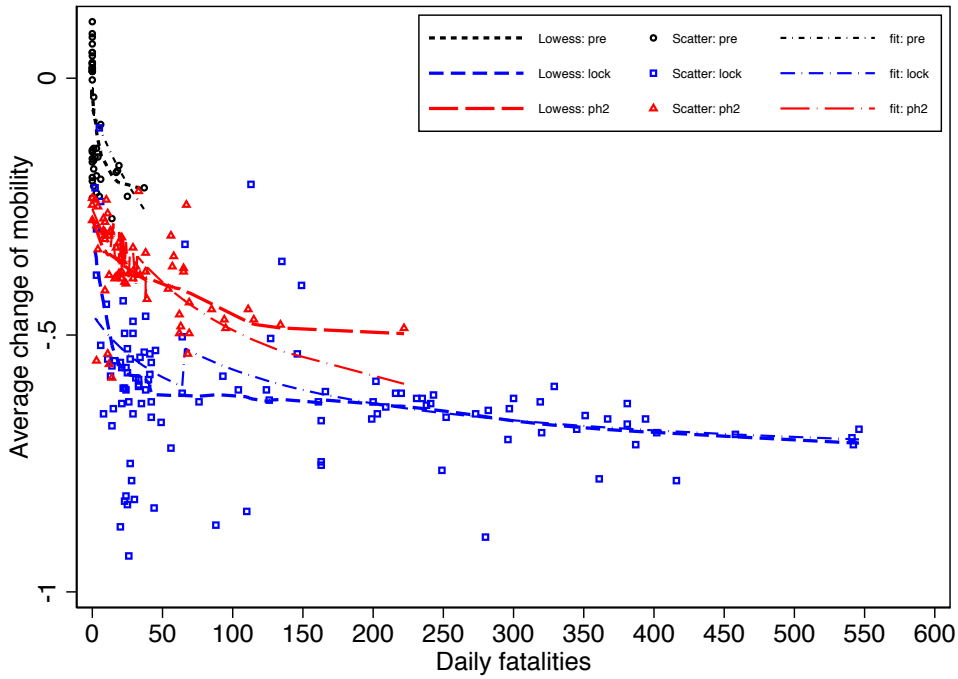

Note: the figure displays the scatter plot of daily fatalities and the average of the Google mobility measures for workplace, transportation and grocery. For each type of mobility, the measure is the change of the number of moves on a given day relative to the same day-of-the-week in the reference period defined as January, 6 – February, 3, 2020. The different markers of the scatter plot identify the three periods for which we have data: Pre-lockdown, Lockdown and Phase2. The figure also plots predictions from locally weighted regressions obtained with the "lowess" Stata command (dashed lines; bandwith=0.8) as well as the predicted values of obtained with the non-linear least square estimates for working days reported in column 4 of Table 2 (dashed-dotted lines).

of the epidemic in the post-lockdown phase, that are efficient with respect to the number of fatalities and to the GDP loss. To this end, we extend the basic SEIR model along many dimensions to the SEIR-HC-SEC-AGE specification described in this section.

First, consistently with the theoretical discussion and the empirical results reported in Section 4, the virus dynamics will be driven by a matrix of net reproduction numbers that are functions of the the containment policies adopted by the government and of the behavioural response of individuals to the development of the virus.

Second, we adopt a multi-risk model that divides the population into 9 age-brackets (from 0-9 to 80+) of which 5 are in working age. The working cohorts are allocated to two-production sectors, characterized by different levels of coworkers proximity, or to inactivity imposed by a containment policy. We have therefore 19 groups with different probabilities of infection, hospitalization and fatality that vary with age, sector and age-specific labor force participation.

Third, the lethality of the virus will have an endogenous component and the dynamics

will include explicit modelling of the policy designed to manage the infectious and control the flows of patients into hospitals. Lethality will be modelled to increase progressively with the saturation of hospitals and to reach a critical point when the available supply of intensive care beds is fully saturated. In this case the observed lethality becomes higher than that implied by the exogenous case fatality ratio (CFR) of COVID-19. In this scenario management of the hospital flows becomes an important policy to reduce mortality. Extensive testing, early detection of the infectious, their placement in domestic quarantine paired with administering medicines can prevent them to reach the stage of symptoms that need hospitalization. Such policy can therefore avoid the creation of "wartime conditions" in hospitals and the ensuing collapse in the quality of medical services. The data from the Northern Italy regions of Veneto and Lombardia reported in Figure 4 hint at the potential importance of this narrative. The pattern of daily deaths from the end of February 2020 to June 11 2020 led to a very different outcome with a total count of 16374 fatalities in Lombardia and 1964 in Veneto (population in Lombardia is 10 millions while in Veneto is 4.9 millions). The figures also illustrate that a difference in the intensity of testing adopted in the two regions led to a much more intense use of domestic quarantine in Veneto paired with a strong control on hospitalization. The initial intensive use of domestic quarantine by Veneto has not led to a successive increase in hospitalization. Over time Lombardia has converged to the policy adopted by Veneto which proved more successful in the containment of the lethality of the disease.

Finally, we complement the epidemiological model with a simple economic structure to model production in the two regions.

5.1 Individual Responses

We first derive the equation describing the number of new exposed (presented as the reduction of the number of susceptible individuals) in the simple case in which there is a single activity, and later extend to the case of multiple activities. Recall that M (defined in equation (1) above) is the number of possible meetings of an individual in a time unit, which we took to be a day.

In our empirical model all the infectious do not initially feel symptoms, but unlike the period in which they were just exposed, they spread the virus for a period that lasts T_{inf} days. After this period they suffer symptoms, that can be mild or severe. Severe patients (SEV) never revert to a state of MILD. MILD patients without proper medical care may turn into Severe. This process occurs after T_{inf} days, in which both infected and infectious have very mild symptoms, and thus do not avoid contacts. Over one day a number $P(V \geq v_t^*)I_t$ of the total infectious I_t is active, and thus meet with susceptible individuals who choose to pursue

Figure 4: COVID-19 in Lombardia and Veneto

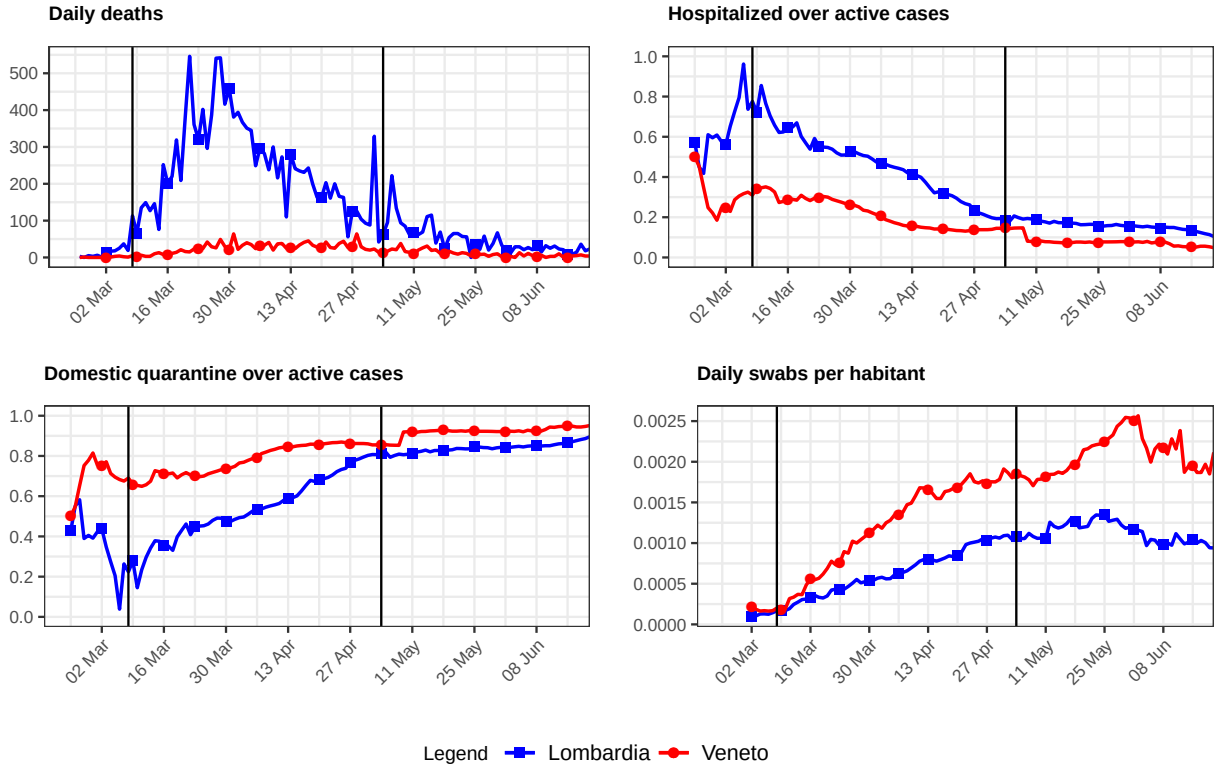

Note: Daily data from Protezione Civile. The vertical bars indicate the start of the Lockdown (March 8), the start of the Phase 2 (May 4).

the activity. A number $Pr(V \geq v_t^*)S_t$ of susceptible individuals is active. When a match occurs, then infection is transmitted with probability $\beta(m)$, the numbers of contacts that an individual makes in a day of generic activity is M. We call, to prepare for the heterogeneous model below,

$$\alpha_t = P(V \geq v_t^*)$$

for the representative agent, single activity case we are considering now. In the general model, we will have $\alpha_t(a, j)$ for group a and activity j at time t. Consistently, in the general model, we shall also have $M(a, b, j)$ as the number of people of type b that a group a meets in activity j.

In conclusion we get:

$$S_{t+1} - S_t \equiv \Delta S_t = -\frac{I_t}{N_t} M\beta(m)\alpha_t^2 S_t \tag{11}$$

Note that, while in the standard SEIR model the time variation of the basic reproduction number depends exclusively on the evolution of the ratio of susceptible to total population, this extension adds two sources of variation. The first one depends on the evolution over

time of the probability with which a contact leads to infection. This ratio is affected by precaution, such as wearing masks, and mutation of the virus aggressiveness that might be related to a number of different factors, such as temperature and humidity. The second one depends on the evolution over time of the average number of contacts made by individuals, that we have seen are related to policies but also to individual responses to the news about the spreading of the virus.

5.2 Endogenous Mortality and Hospital Management

After having included the behavioral responses in the determination of R_t and in the dynamics of susceptible and exposed individuals, we extend the model to have an endogenous component of lethality that becomes larger as hospitals become crowded. This component explodes when the Intensive Care capacity is fully saturated; in this case all patients in need of Intensive Care but not able to access it, die. Differently from (Favero, 2020), however, in our model hospital saturation increases mortality even before the ICU capacity is reached. Within this framework, we introduce testing, which leads to domestic quarantine of the infectious with mild symptoms. Domestic quarantine, paired with pharmacological treatment, can stop them from reaching a stage requiring hospitalization. The ensuing reduction in hospital saturation has in turn an important impact on reducing the endogenous component of lethality.

The infected move from the compartment of the infectious to two different compartments: those with mild symptoms, $MILD_t$, and those with severe symptoms, SEV_t. The allocation to these groups is controlled by two probabilities: p^{mild} and $\left(1-p^{mild}\right)$. Testing allows to detect a share δ of those destined to become MILD; they thus become detected, $MILD_t^D$ while $(1-\delta)$ become undetected, $MILD_t^U$. Detection and associated medical care reduces the length of the period in which agents are infectious from T_{inf} to $T_{\text{inf}_0} < T_{\text{inf}}$. The same applies to the infectious who are destined to become Severe. As a consequence of the severity of symptoms, there are no Severe undetected after T_{inf} days in which they are virtually asymptomatic.

The mild infected either recover – after periods of duration respectively of $T_{srec,U}$ and $(T_{srec,D})$ days – or their condition becomes severe and they require hospitalization, after a period of duration $T_{shosp,U}$ $(T_{shosp,D})$ days. The probability of becoming severe is higher for the undetected than for the detected: $p^{M2Sev,U} > p^{M2Sev,D}$.

So the dynamics of the Infectious in daily data is as follows:

$$
\begin{aligned}
\Delta I_t &= \left(\frac{1}{T_{inc}}\right) E_{t-1} - (1-\delta)\left(\frac{1}{T_{\inf}}\right) I_{t-1} - \delta\left(\frac{1}{T_{\inf_0}}\right) I_{t-1} \\
\Delta MILD_t^U &= p^{mild}(1-\delta)\left(\frac{1}{T_{\inf}}\right) I_{t-1} - \left(\frac{1}{T_{srec,U}}\right) MILD_{t-1}^U - p^{M2Sev,U}\left(\frac{1}{T_{shosp,U}}\right) MILD_{t-1}^U \\
\Delta MILD_t^D &= p^{mild}\delta\left(\frac{1}{T_{\inf_0}}\right) I_{t-1} - \left(\frac{1}{T_{srec,D}}\right) MILD_{t-1}^D \\
&\quad -p^{M2Sev,D}\left(\frac{1}{T_{shosp,D}}\right) MILD_{t-1}^D \\
\Delta SEV_t &= (1-p^{mild})\left((1-\delta)\left(\frac{1}{T_{\inf}}\right) + \delta\left(\frac{1}{T_{\inf_0}}\right)\right) I_{t-1} - \left(\frac{1}{T_{shosp}}\right) SEV_{t-1}
\end{aligned}
$$

With testing and early detection, patients are cared at home and hospitals congestion is reduced. MILD patients who become severe and are hospitalized recover after a period of $(T_{shd,U} - T_{shosp,U})$ days. All severe patients become hospitalized after T_{shosp} days. Severe hospitalized either recover after $(T_{shd,U} - T_{shosp,U})$ days with probability p^{ic} or they worsen with probability $(1 - p^{ic})$ and require intensive care after $T_{hosp-ic}$ days. Patients needing ICU may die or recover. When ICU is available and there is no hospital congestion mortality in ICU generates the same fatality rate of a standard SEIR model, p^{fat}. However, mortality in ICU increases with hospital congestion. This increase is modelled by a logistic function of total hospitalization. The parameter k in the logistic is calibrated in such a way that the endogenous mortality probability is zero under normal conditions and it increases with hospital saturation. When ICU is fully saturated, mortality explodes as all patients in need of ICU who do not find availability succumb. Those patients in ICU who recover, leave ICU after $(T_{shd} - T_{hosp-ic})$. Those who do not recover die after $(T_{sd} - T_{shosp-ic})$. Those who need ICU and do not find it available, die immediately.

At the end of each day the population decreases because of fatalities, while the stock of recovered grows by the amount of those who survive having had mild or severe symptoms, with or without the need of IC. The cycle starts again in the next day. Finally, it is worth noting that the specification of the endogenous component of mortality could be enriched to include the effect of cures, other than the vaccine, that are proved to be effective in reducing the mortality of the disease.

The model is represented graphically in Figure 5 and a detailed description of all the equations is given in the Online Appendix.

Figure 5: Flowchart of the SEIR-HC model

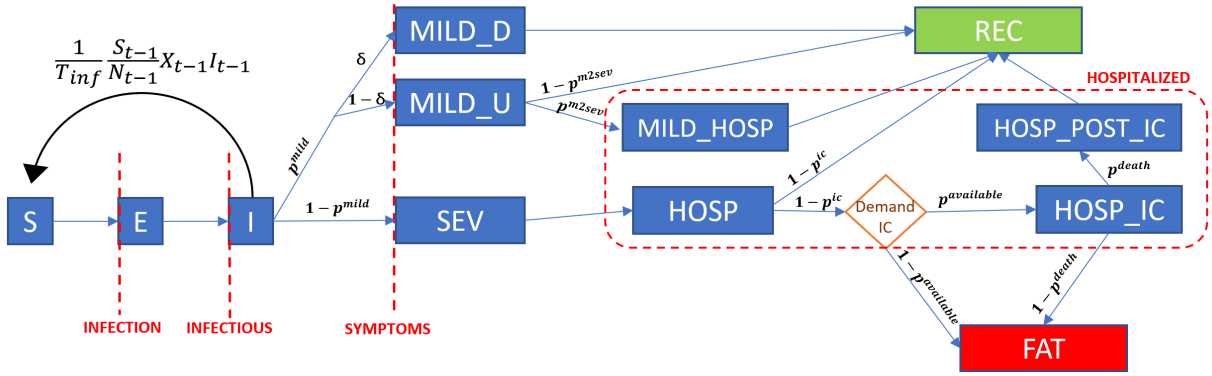

Note: Description of the dynamic transitions of a subject in the SEIR-HC model (Favero, 2020).

5.3 Extension to Multi-sector

To build our final SEIR-HC-SEC-AGE model, we extend the structure of the SEIR-HC model to allow for 9 age brackets of ten-years groups, from 0–9, 10–19 ... to 80+ years of age, and for two sectors in which subjects between age 20 and 65 have the possibility to work.[12] The two sectors differ because of the risk of becoming infected faced by the workers who operate in them. In this extended model the dynamics of transitions of patients that are exposed to the virus is qualitatively the same as the one of the SEIR-HC model described in Figure 5. The crucial difference is that in the extended model the reproduction number is not the same for the entire population and varies instead with the age, employment status and sector of the infectious subject and of the subjects that become exposed to her/him.

Each age bracket between 20 and 69 years of age is split into three separate groups. The first two groups include individuals who work respectively in the low-risk or in the high-risk sectors; the third and last group include individuals in working age that are not part of the labor force. This amounts to 5 age groups of active in the low-risk sector, 5 age groups of active in the high-risk sector, and 5 age groups of inactive. In addition to these 15 groups there are two age groups of inactive under 20 and 2 age groups of inactive over 69. Thus, we have in total 19 groups, $A \equiv \{1, 2, \ldots, 19\}$, with generic term $a \in A$. Workers correspond to the elements $\{3, \ldots, 12\}$ with $\{3, \ldots, 7\}$ in the low-risk sector and $\{8, \ldots, 12\}$ in the high-risk sector. The set $\{13, \ldots, 17\}$ indicates the inactive groups in the five active age brackets. The number of age groups of workers is $L = 5$, and so $3L = 15$ is the number of classes of

[12] As explained below in Section 6.2, these are the age brackets for which Ferguson et al. (2020) estimate biological and epidemiologial parameters of Covid-19, and these is why we adopt the same categorization. Labor participation rates are allowed to change in these age brackets in line with available statistics for the two regions as explained in Section 6.1.

workers as distinct by age, risk sector and activation. The basic reproduction number will therefore be replaced by a matrix, which is allowed to differ among these groups and as a function of the level of activity of the corresponding workers (for example, a worker in the high-risk sector does not infect many people if he is not active). This is a crucial feature of the extended model.

5.4 Dynamic Model

Moving from the model for the single agent to the model for heterogenous groups, we introduce X_t, a time-varying components, shared by all groups, that reflects (i) the initial value and the change in the probability that a contact with an infectious leads to an infection, and (ii) the average change in the number of contacts in the population determined by the average behavioural response to the virus. The equation for the exposed is then a system of equations for each age group $a \in A$ of the form:

$$\Delta E_t(a) = E_{t-1}(a) - \frac{1}{T_{Inc}} E_{t-1}(a) + \frac{1}{T_{Inf}} X_{t-1} \sum_{b \in A} \frac{I_{t-1}(b)}{N_{t-1}} R(b,a) S_{t-1}(a) \tag{12}$$

Similarly, the equation for the infectious becomes the system:

$$\Delta I_t(a) = I_{t-1}(a) + \frac{1}{T_{Inc}} E_{t-1}(a) - \frac{1}{T_{Inf}} I_{t-1}(a) \tag{13}$$

and that for the susceptible individuals is:

$$\Delta E_t(a) = -\frac{1}{T_{Inf}} X_{t-1} \sum_{b \in A} \frac{I_{t-1}(b)}{N_{t-1}} R(b,a) S_{t-1}(a) \tag{14}$$

The same generalization applies to modelling all the compartments considered in the model with endogenous mortality.

5.5 Activity Levels per Sector

To model the effects of policies that restrict the access to work of specified categories of workers we need to model how the basic reproduction matrix depends on the level of activity. We will focus in the following on the sub-matrix defining the reproduction rates within the workforce, that is the sub-matrix that describes how many infected workers of class a are generated by workers of type b; here a and b are generic elements of the set of workers, indexed in the set $\{1, 2, , \ldots, 3L\}$.

We denote $\alpha : \{1, 2, \cdots, 3L\} \times \{0, 1\} \to [0, 1]$ the level of activity, with $\alpha(a, 1)$ the level of activity of class a (for example, $a = 9$ indicates individuals of age 30 to 39 in the high-risk

sector); the fraction of workers allowed to work and not add to 1: $\alpha(a,0) = 1 - \alpha(a,1)$. We also denote $R(a,b;i,j)$ with $a,b, \in \{3,\ldots,12\}$ and $i,j \in \{0,1\}$ the number of workers of type b that a worker of type a infects when a is i-active (that is, active if $i=1$ and not active if $i=0$) and b is j-active. Finally we denote $s(a)$ the (high, low or inactive) risk sector of the class a; for instance $s(3) = Low$, $s(10) = High$. Thus we define the basic reproduction matrix at level α of activity as:

$$R(a,b;\alpha) = \sum_{(i,j)\in\{0,1\}^2} R(a,b;i,j)\alpha(a,i)\alpha(b,j) \tag{15}$$

We assume:

1. $R(a,b;i,j) = Risk(s(a))$ if $s(a) = s(b)$ and $(i,j) = (1,1)$
2. $R(a,b;i,j) = Tr$ if $s(a) \neq s(b)$ and $(i,j) = (1,1)$
3. $R(a,b;i,j) = Iso$ if $(i,j) \neq (1,1)$

The first condition requires that the BRM of a on b when both are active and in the same sector only depends on the sector (and not on the age of a and b): so $Risk(L)$ for the low-risk sector and $Risk(H)$ for the high-risk sector. The second condition requires the value to be the same for two active workers, but working in different sectors (Tr is suggestive of the means of transportation that they share when going to work even if the do not affect each other during work). The third condition requires that if one of the two workers is not active (no matter who that is among the two) then the BRM value is equal to a common value Iso which is suggestive of isolation.

Under these conditions the matrix $R(a,b;\alpha)$ is a very simple combination of the $3L \times 3L$ activation matrix $A(\cdot;\alpha)$:

$$A(a,b;\alpha) \equiv \alpha(a,1)\alpha(b,1) \tag{16}$$

and the five-values parameter $\rho \equiv (Risk(L), Risk(H), Risk(In), Tr, Iso)$. For example $R(a,b;\alpha)$ is equal to $Risk(H)A(a,b;\alpha)$ when $s(a) = s(b) = High$.

The value of α for inactive individuals is constrained to reflect the inactivity condition:

$$\text{for all } a \in \{13,\ldots,17\} : \alpha(a,0) = 1. \tag{17}$$

In view of the constraint (17), in the description of the calibration of parameters and policies we focus on the $2L$ levels of activity of the workforce. We denote α_{min} the minimum level of activity of each active class, and with $\mathbf{1}$ the vector of activity corresponding to normal conditions.

In the calibration of the parameter ρ, we set the level of activity corresponding to normal and minimum activity as:

$$R_{normal} = R(a, b; \mathbf{1}); R_{lock} = R(a, b; \alpha_{min}) \tag{18}$$

We assume that the values of the reproduction matrix for the inactive is the same as the one between workers in different sectors:

$$Risk(In) = Tr \tag{19}$$

Given the parameter restriction and the model, we calibrate parameters to match the number of fatalities in a given region (for instance, Lombardia or Veneto).

5.6 Adding Economics to the Model

For given demographic and epidemiological parameters, the SEIR-HC-SEC-AGE model described in the previuos section produces a set of public health effects of Covid-19 that depend on the behavioral response and on the age brackets and sectors that are allowed to go back to work according to the post Lockdown policy that the authority will decide to implement. Our goal is to compare public health effects and economic effects of different possible policies.

A policy π is formally defined as a vector with ten elements, each one corresponding to one of the five potentially active age brackets in each of the two sectors. Each element of this vector specifies the fraction of the workforce that is allowed to go back to work in the corresponding age bracket/sector. Table 3 describes five of these policies in which we are specifically interested.

Table 3: A set of possible post lock down policies

	Low-risk sector Age brackets					High-risk sector Age brackets				
Policy	20-29	30-39	40-49	50-59	60-65	20-29	30-39	40-49	50-59	60-65
π = LOCK	0.6	0.6	0.6	0.6	0.6	0.6	0.6	0.6	0.6	0.6
π = SEC	1	1	1	1	1	0.6	0.6	0.6	0.6	0.6
π = AGE	1	1	1	0.6	0.6	1	1	1	0.6	0.6
π = AGE_SEC	1	1	1	0.6	0.6	1	0.6	0.6	0.6	0.6
π = ALL	1	1	1	1	1	1	1	1	1	1

Note: In this table, an entry equal to 1 (0.6) means that the entire (60% of the) labor force of the correspondent age bracket and sector is activated.

Defining with t^* the day in which the authority intends to start Phase III (e.g., September 1 for Italy in our simulation), Policy "LOCK" is defined as going back after t^* to a Lockdown with the minimum set of workers that were employed during the March 2020 Lockdown,

which is on average equal to about 60% of the labor force according to Barbieri et al. (2020). Policy "SEC" is based on sending back to work after t^* all the labor force of the low-risk sector, and only the strictly needed minimum in the high risk sector, which incidentally includes health and education workers according to Barbieri et al. (2020). Policy "AGE" uses only age as the criterion to decide who is allowed to resume activities after t^*: under this policy all workers between 20 and 49 years of age go back to work independently of the sector, while only 60% of the older workers is allowed to be productive in both sectors. Policy "SEC_AGE" is representative of what a mixed policy could look like, using both the age and the sector criteria: all workers under 50 in the low-risk sector and under 30 in the high-risk sector resume activities, while 40% of the older workers in all sectors has to stay home. Finally, Policy "ALL" sends back to work all those who were working before the Covid-19 outbreak. Note that schools, even if they are part of the risky sector, are assumed to reopen with at least the minimum set of workers allowed by each policy. Of course, many more policies can be defined in a similar way, but these are the emblemeatic ones in which we are interested. Our framework could be easily adjusted to consider also policies differentiated by geographic area.

Using the SEIR-HC-SEC-AGE model described in previous sections we can associate to every policy π and region r its public health effects that we summarize with the total number of fatalities in the first year after t^*:

$$TOT\_FATr, \pi = \sum_{t=t^*}^{t^*+365} REM\_FAT_{t,\pi} \tag{20}$$

As for the economic effects, we summarize them as a function of the fraction of the labor force that is not allowed to work under a given policy π. We are fully aware that a complete characterization of the economic costs of the Covid-19 pandemic would require a more sophisticated and detailed dynamic macroeconomic model, which we leave for future extensions of this project. For the time being, given the urgency of comparing the economic effects of different post lockdown strategies, we believe that estimating these consequences as a function of the fraction of the labor force that cannot work is sufficiently informative at least about the orders of magnitude. Specifically we assume that the GDP of region r, denoted as $\mathbb{Y}_r$, is a Cobb Douglas function of labor $\mathbb{L}_r$ and capital $\mathbb{K}_r$,

$$\mathbb{Y}_r = A\mathbb{K}_r^{1-\eta}\mathbb{L}_r^{\eta},$$

so that the percent GDP change induced, ceteris paribus, by a variation $d\mathbb{L}_r$ of the employed

labor force is

$$\Delta \mathbb{Y}_r \approx \frac{d\mathbb{Y}_r}{\mathbb{Y}_r} = \eta \frac{d\mathbb{L}_r}{\mathbb{L}_r} \tag{21}$$

which is a negative number if $d\mathbb{L}_r < 0$. Each post lockdown policy π will produce a decline $d\mathbb{L}_{r,\pi}$ of the employed labor force and thus a corresponding percent GDP loss $\Delta \mathbb{Y}_{r,p}$ according to equation (21). This GDP loss is the measure of the economic effects of the interaction between policy π and Covid-19 that we consider.

Within this framework we aim at making two contributions. First, we want to characterize an efficient set of policies. Second, we want to compare between themselves and against the efficient frontier the five stereotypical post lockdown policies described in Table 3.

6 Calibration of the Model

The calibration of the SEIR-HC-SEC-AGE model requires giving values to different sets of parameters that are described in this section. The relevant dates for the simulation are described in Table 4.

Table 4: Relevant dates for the simulation

	Observed Past				Simulated Future	
	Appearance of the virus	Beginning of observed data	Beginning of the lock down	Start of Phase II	Start of Phase III policies $= t^*$	End of simulation $= t^* + 364$
Date	January 1 2020	February 24 2020	March 8 2020	May 4 2020	September 1 2020	August 31 2021

We assume that in both region the virus SARS-Cov-2 arrived at the beginning of 2020 so that the first infectious subjects is observed on January 1, 2020. The available data on the diffusion of Covid-19 in Italy, published by the Protezione Civile, are available from February 24, 2020 and are continuously updated.[13] The first lock down has been introduced by the Italian government on March 8, 2020.

The government has modified the Lockdown policy starting with a partial release of the measures, the so-called Phase II, on May 4, 2020. We simulate the effects of the hypothetical Phase III policies starting from September 1, 2020. We end the simulation after one year, on August 31, 2021.

[13]The data can be downloaded from https://github.com/pcm-dpc/COVID-19.

Table 5: Fraction of the population and labor force participation in each age bracket

	Age brackets								
	0-9	10-19	20-29	30-39	40-49	50-59	60-69	70-79	80+
Lombardia									
Population	0.088	0.094	0.098	0.118	0.158	0.156	0.118	0.099	0.071
Participation			0.494	0.771	0.832	0.804	0.235		
Veneto									
Population	0.085	0.096	0.098	0.112	0.156	0.161	0.121	0.100	0.071
Participation			0.497	0.751	0.826	0.794	0.236		

Note: The table reports the fraction of the population in each age bracket and the labor force participation rates for the brackets between age 20 and age 69 in Lombardia and Veneto. The SEIR-HC-SEC-AGE assumes, in line with the available evidence, no significant labor force participation in the other age brackets. The total population is 10 ml. in Lombardia and 4.9 ml. in Veneto (Source: ISTAT).

6.1 Demographic Parameters and Labor Share

The distribution of the population and of the labor force participation rate in the nine age brackets[14] that we consider for the two regions is taken from ISTAT and is reported in Table 5. As expected Lombardia and Veneto have a similar distributions, with a slightly higher fraction of over-50 in Veneto (45.3%) than in Lombardia (44.4%). The total population of the two regions is instead significantly different: 10 ml. in Lombardia and 4.9 ml. in Veneto.

In order to compute the GDP loss we need to calibrate the parameter representing the labor share, and thus the coefficient that maps the loss of employment due to Covid-19 into a GDP loss. For the value of this parameter we follow Torrini (2016), who estimates it to be 0.65 for the Italian economy. In the absence of specific information about this parameter for the two regions that we consider, we use this estimate for both Lombardia and Veneto.

6.2 Covid-19 Parameters

There are two sets of relevant parameters describing the health consequences of Covid-19 for an exposed subject. We take both these sets from Ferguson et al. (2020). An obvious caveat in considering these parameters is that they are estimated on the basis of data from China adjusted to predict US and Great Britain targets. We cannot exclude that the corresponding values for Lombardia and Veneto are different. However, the estimates of Ferguson et al. (2020) have been confirmed by follow up research for different regions in the world.[15] We hope to be able to improve this parameter estimates if and when reliable data based on random testing for these two regions will become available. In any case, we do not expect

[14] See Footnote 12.

[15] We have also evaluated the robustness of our results using the Covid-19 parameters calculated by the Center of Deseases Control (CDC) for the U.S. (Garg, 2020) and results are reported in the Online Appendix.

that the comparison of the effects of the different policies should be particularly sensitive to reasonable changes of these parameters, at least in terms of first order consequences.

Table 6: Health effects of Covid-19 by age bracket

	Age brackets								
	0-9	10-19	20-29	30-39	40-49	50-59	60-69	70-79	80+
p^{sev}	0.001	0.003	0.012	0.032	0.049	0.102	0.166	0.243	0.273
p^{ic}	0.05	0.05	0.05	0.05	0.063	0.122	0.274	0.432	0.709
p^{fat}	0.00002	0.00006	0.0003	0.0008	0.0015	0.006	0.022	0.051	0.093

Note: the table reports for each age bracket the probability of hospitalization, p^{sev}, the probability of needing intensive care if hospitalized, p^{ic} and the probability of death p^{fat} for a subject exposed to Covid-19 infection. Source: Ferguson et al. (2020).

The first set of Covid-19 parameters defines the probability of hospitalization, p^{sev}, the probability of needing intensive care if hospitalized, p^{ic}, and the probability of death p^{fat} by age bracket and is described in Table 6. The values of all these probabilities clearly indicates that Covid-19 is considerably more dangerous for the old, with a pronounced increase of risks for subjects with an age greater than 50.

The second set of Covid-19 parameters that we need describes the lags of the transitions between states of the disease in the basic SEIR model; they are described in Table 7. As by now well known, a characteristics that makes SARS-Cov-2 particularly nasty is the number of days in which a subject may be infectious without showing symptoms, which is on average $T_{inf} = 2.9$. $T_{inc} = 5.2$ is instead the average number of days of incubation before showing symptoms. The period going from the day in which the first symptoms appear to the day of recovery is usually of $T_{srec} = 11.1$ days for a Covid-19 patient, while in case of death, this event occurs $T_{sd} = 17.8$ days after the appearance of symptoms. Hospitalization, if it is needed, occurs typically $T_{shosp} = 5$ days after symptoms, while the period from symptoms to hospital discharge in case of hospitalization is of $T_{shd} = 22.6$ days.

Table 7: Transition lags in the evolution between illness states of Covid-19

	Infectious without symptoms T_{inf}	Incubation without symptoms T_{inc}	Symptoms to recovery T_{srec}	Symptoms to death T_{sd}	Symptoms to entry in hospital T_{shosp}	Symptoms to discharge from hospital T_{shd}
Days	2.9	5.2	11.1	17.8	5	22.6

Note: the table reports the number of days for each transition between illness states of Covid-19. Source: Ferguson et al. (2020).

We also calibrate, to match the evolution of daily fatalities, $T_{shospU} = T_{shospD} = T_{shosp} = 5$ as well as $T_{srecU} = T_{srecD} = T_{srec} = 11.1$, i.e. the number of days before hospitalization and

the recovery time is common across types of people. A fraction of hospitalized patients requires an IC bed after $T_{hosp-ic} = 3$ days and if they survive they stay other $T_{ic-rec} = 7$ days before they completely recover. Finally, $T_{sd-hosp} = 12.8$ and $T_{shd-inf} = 17.6$.

6.3 Availability of Beds in Intensive Care

The SEIR-HC-SEC-AGE model makes the constraint in the availability of IC beds endogenous. When this constraint is binding, all subjects who need intensive care and do not find it become fatalities. Figure 6 illustrates how the constraint has operated in the two regions during the period for which data are available.

Figure 6: The IC availability constraint in Lombardia and Veneto

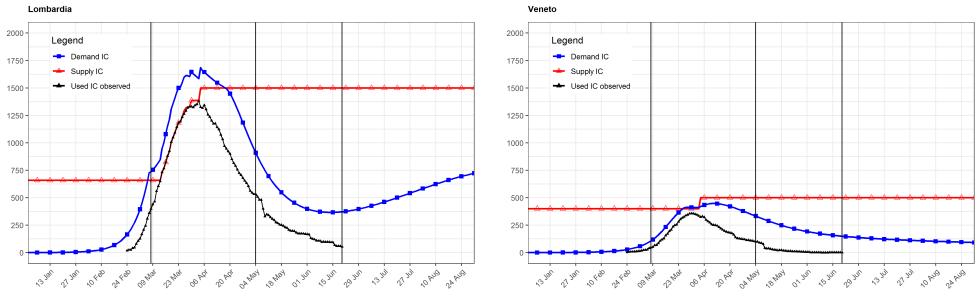

Note: The figure reports, respectively for the two regions, the simulated demand for IC beds due to Covid-19, the observed number Covid-19 patients in IC and the observed number of patients that were effectively hospitalized in IC. The vertical bars indicate the start of the Lockdown (March 8), the start of the Phase 2 (May 4) and the end of data availability (June 20). The observed series were downloaded from https://github.com/pcm-dpc/COVID-19 for the used IC and from https://www.dropbox.com/s/skabm9ct71qud32/ICU%20beds%20statistics.xlsx?dl=0 for the supply of IC.

In Lombardia (left panel), given the initial very fast diffusion of the virus and the number of available IC beds, the constraint started to bite very quickly. These facts are responsible for the explosion of fatalities in this region which is displayed in the left panel of Figure 8. Even if Lombardia made a major effort to increase the supply of IC beds, the constraint continued to bite for a long time. In Veneto instead, the demand of IC is simulated to be higher than the supply in only one relatively short period.

6.4 BRN of Covid-19 by Age and Sector

It is well known that every variant of the SEIR model is very sensitive to the basic reproduction number. In the case of the SEIR-HC-SEC-AGE extension that we have designed, the calibration of BRN is further complicated by the need to set different values for different combinations of age, sector and working status of an infectious subject and of the susceptible subjects that enter in contact with him/her, which requires to calibrate a 19×19 Basic Reproduction Matrix (BRM).

Moreover, given the presence of a behavioural response, we have to calibrate how this initial matrix evolves over time to generate a time varying R_t matrix for the periods for which we have data: the period before the Lockdown, the period of the Lockdown and the period of the Phase 2. Finally, we will do out-of-sample simulations of the alternative policies for the Phase 3.

6.4.1 Calibration of BRN by Age and Sector

The 19×19 BRM is driven by the parameters in the vector ρ. As $R_0 = \beta_0 M_0$ and β_0 is common to all the elements of the BRM, then the parameters in the vector ρ are not independent, as their ratio reflects the relative number of contacts between subjects at work, on transports, doing grocery and at home. The calibration of these four parameters is however simplified by the fact that, with the auxiliary information described below, they can be all set as a linear function of a single parameter, $Risk(work)$, which captures the number of contacts in an average working site. So, by calibrating $Risk(work)$ in a way such that the model matches the fatalities observed respectively in the two regions, we calibrate also the other parameters that are linearly related to $Risk(work)$.

The first type of auxiliary information that is needed to implement this strategy concerns the estimated number of contacts for the Italian population which we obtained from the official documentation released by the government to justify the rules for the Phase 2.[16] This information suggests that the average number of contacts on transportation is 65% of the number of contacts in an average working place, while the correspondent number when not at work or not on transports is 60%. Therefore we set $Tr = 0.65 * R(work)$ and $Iso = 0.60 * R(work))$.

We then discipline the remaining parameters of the vector ρ, $Risk(L)$ and $Risk(H)$, using the evidence in Barbieri et al. (2020) who report an index of proximity for workers operating in different sectors of the Italian economy. Sectors with higher proximity indices are those in which spreading of the virus is likely to be higher. Based on the evidence in their Table 3, we compute the proximity index for the sectors above and below the mean proximity index. We then assume that the percent difference between $Risk(H)$ and $R(work)$ is equal to the percent difference between the proximity index for sectors above the mean index and the mean index itself. This difference is equal to 18%. Similarly for the percent difference between $Risk(work)$ and $Risk(L)$, which is equal to 12%.

[16] Specifically, we use the numbers in Table 1 of the document provided at this link `https://www.ilmessaggero.it/uploads/ckfile/202004/Riaperture_report_27222237.pdf?`, that is based on original data from the "Istituto nazionale Assicurazione Infortuni sul Lavoro (INAIL)" and from Mossong et al. (2008).

6.4.2 Evolution within Sample of BRN

Given R_0, R_t will evolve as a function of the number of infectious I_{t-1} and of the cost of containment policies K_t according to:

$$R_t = \frac{S_{t-1}}{N_{t-1}} \frac{\beta_{t-1}}{\beta_0} \left(\frac{\frac{\overline{V}}{C\tilde{p}} - \frac{K_t}{C\tilde{p}}}{I_{t-1} + \frac{\overline{V}}{C\tilde{p}}} \right)^2 R_0$$

To determine the parameters in the term $\left(\frac{\frac{\overline{V}}{C\tilde{p}} - \frac{K_t}{C\tilde{p}}}{I_{t-1} + \frac{\overline{V}}{C\tilde{p}}} \right)$ we use the estimates of the behavioural response of Grocery moves in the third column of Table 2 of Section 3. We pick the parameter estimates for Grocery because they refer to an activity that can be chosen more freely by an individual, differently than workplace and transportation activities that may be constrained by the legal possibility to work or by interruptions of transportation services during Lockdown or the Phase 2. Indeed Grocery was never prohibited, provided that a minimum distance could be maintained between individuals inside the shops or in their vicinity.

We therefore have, respectively for Lombardia and Veneto,

$$\left(\frac{\frac{\overline{V}}{C\tilde{p}} - \frac{K_t}{C\tilde{p}}}{I_{t-1} + \frac{\overline{V}}{C\tilde{p}}} \right) = \frac{623.80 - (163.26 Lock + 114.47 Phase2)}{I_{t-1} + 623.80}$$

$$\left(\frac{\frac{\overline{V}}{C\tilde{p}} - \frac{K_t}{C\tilde{p}}}{I_{t-1} + \frac{\overline{V}}{C\tilde{p}}} \right) = \frac{540.79 - (163.26 Lock + 114.47 Phase2)}{I_{t-1} + 540.79}$$

For the reasons explained in Section 3, the empirical counterpart of I_{t-1} in the simulation model is a seven-day backward looking moving average of observed daily mortality and *Lock* and $Phase2$ are two dummies for the Lockdown and the Phase 2, respectively.

To later understand the role of containment policies it is useful to define the value of R_t within each regime in an hypothetical situation in which the policy is implemented in the absence of fatalities associated to the virus, and thus shutting down the behavioural response factor. We define this value as

$$R_{0,eq} = \frac{\beta(m)_{t-1}}{\beta(m)_0} \left(\frac{\frac{\overline{V}}{C\tilde{p}} - \frac{K_t}{C\tilde{p}}}{\frac{\overline{V}}{C\tilde{p}}} \right)^2 R_0$$

Its determination requires to calibrate the ratio $\frac{\beta(m)_{t-1}}{\beta(m)_0}$ which is set to 1 in the pre-Lockdown period, reduced to 0.97 from March 8 until June 30 and to 0.8 after this date. This reduction is a consequence of the precaution measures (compulsory masks and social distancing during

contacts) introduced with the Lockdown and maintained during Phase 2.

6.4.3 Endogenous Mortality and Hospital Flows

Testing policies are calibrated to be initially different for Lombardia and Veneto, but they are forced to converge after the Lockdown, in line with the evidence from the data. Therefore, δ is calibrated permanently to 0.3 for Veneto while it is set initially to 0 in Lombardia and successively increased to 0.25 during Lockdown.

To capture a testing policy designed to control hospitalization flows we set $T_{\text{inf}\,0} = T_{\text{inf}}$. To match the evidence on the stability of the ratio of quarantined at home to total infected in Veneto, we set the probability with which a detected MILD requires hospitalization to zero. To match hospital flows, the probability $p^{fat}\gamma$ with which the MILD Undetected become Severe and need hospitalization is set to 0.9.

6.5 Calibration of Risk at Work

Figures 7 and 8 show that our calibration of $Risk(work)$ and of the other related parameters produces a very good match between simulated and observed fatalities. What is crucial for the model to successfully match the two very different patterns of mortality in Lombardia and Veneto is the difference in the endogenous fatality rates of Covid-19 for the two regions. As argued in Section 5.2, this heterogeneity is generated by the different management policies of the hospital flows, and by the associated unequal degrees of hospital and ICU saturation.

Figure 7: Simulated and observed total fatalities

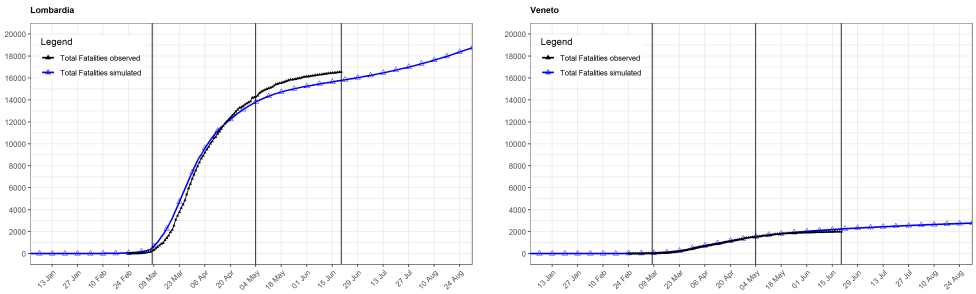

Note: The figure reports, respectively for the two regions, the simulated and observed numbers of total fatalities due to Covid-19. The vertical bars indicate the start of the Lockdown (March 8), the start of the Phase 2 (May 4) and the end of data availability (June 20). The observed series were downloaded from https://github.com/pcm-dpc/COVID-19.

The BRMs for the pre-Lockdown period that result from the calibration for Lombardia and Veneto are respectively displayed in the left and right panels of the Appendix Figure A–1. As expected, in each region the reproduction number for interactions among workers in

the low-risk sector is smaller than for the interactions involving non-active subjects and even smaller than in the high-risk sector. More interestingly, to match the observed mortality in the two regions, in each pair of corresponding blocks of the two matrices the relevant R_0 must be set to a considerably higher value for Lombardia. This difference reflects local factors such as the density in the population which is higher in Lombardia (422 inhabitants per Km^2) than in Veneto (267 per Km^2).

Figure 8: Simulated and observed daily fatalities

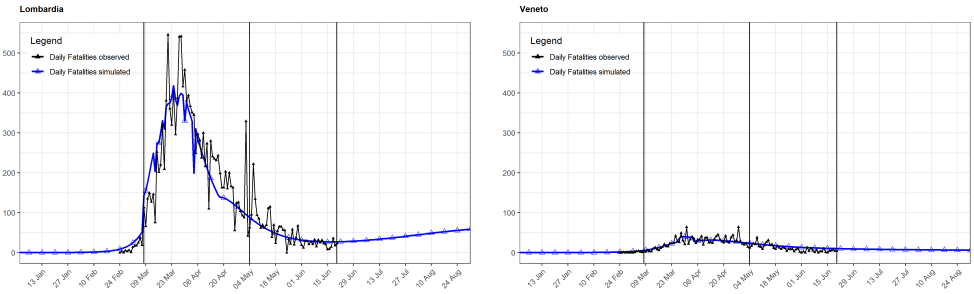

Note: The figure reports, respectively for the two regions, the simulated and observed numbers of daily fatalities. The vertical bars indicate the start of the Lockdown (March 8), the start of the Phase 2 (May 4) and the end of data availability (June 20). The observed series were downloaded from https://github.com/pcm-dpc/COVID-19.

In the Lockdown regime the equivalent concept of R_0 is $R_{0,eq}$ (see section 6.4.2), which is a summary statistic for the R_t that would prevail in that regime in the counterfactual situation of no fatalities associated to the virus. In this situation there would be no behavioural response and R_t would be constant over time. The equivalent BRMs during the Lockdown for the two regions are reported in the two panels of the Appendix Figure A–2. The entries in these matrices are remarkably lower across the entire population with respect to the pre-Lockdown values in Figure A–1. Relatively high values are observed only for the working population because, as already mentioned, during Lockdown a minimum fraction of workers (60% according to Barbieri et al., 2020) was allowed to work. Therefore the $R_{0,eq}$ for the working population during Lockdown is produced by the same activation matrix prevailing in the pre-Lockdown regime for 60% of the population.

Figure 9 displays instead the evolution over time of the average R_t, which is determined by the behavioural response to fatalities and to the policies that we calibrate using the estimates of Table 2 in Section 3 (se also Section 6.4.2). This behavioural response determines a slight decrease of the average R_t in the pre-Lockdown period, when fatalities become positive but social distancing is not yet universally common in the population. At the beginning of the Lockdown we observe a sharp decrease of R_t as a reaction to the introduction of the containment policy, followed by a further reaction induced by the behavioural response to

fatalities. When fatalities level off at the end of March and then decline, the average R_t begins to increase but it never goes back to initial values, since fatalities do not go back to zero even during Phase 2 and until the observed data are available.

Figure 9: Simulated average R_t

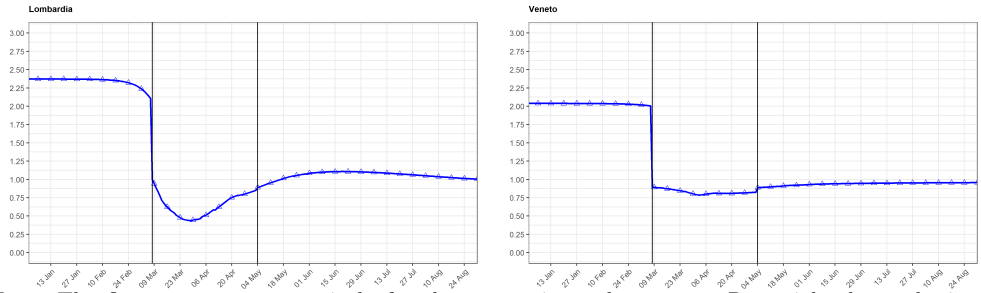

Note: The figure reports, respectively for the two regions, the average R_t, weighted to take into account the population structure. The vertical bars indicate the start of the Lockdown (March 8) and the start of the Phase 2 (May 4).

7 Results of Policy Simulations

We simulate the model to predict the effects of the hypothetical policies that could be adopted in the two regions as of t^* = September 1, 2020. We run the simulation for 365 days, under the assumption that by August 31, 2021 a vaccine or a therapy for Covid-19 will be available. We present our results in two sections: the first one describes the construction of the BRM equivalent matrices for the different policies, while the second one illustrates the results of the out-of-sample simulations.

7.1 Construction of Policies

Since each policy has its own workers activation vector, also the corresponding BRMs differ between policies. The parametrization of these matrices is however simplified by the fact that they are divided in blocks characterized by the same $R_{0,eq}$, because they refer to subjects with similar types of interactions from the viewpoint of the Covid-19 diffusion. The values of $R_{0,eq}$ in the various blocks are determined by the combination of the activation matrix $M(a, b; \alpha)$ with the basic reproduction numbers in the vector $(Risk(L), Risk(H), Risk(work), Tr, Iso)$.

The two panels of the Appendix Table A–1 report, respectively for Lombardia and Veneto, the values of the relevant $R_{0,eq}$ corresponding to each policy and type of interaction. The last column in both tables report the mean $R_{0,eq}$ for each policy, obtained as an average of the policy/interaction specific $R_{0,eq}$, weighted by the size of the corresponding population. We also report, as an illustrative case, the full $R_{0,eq}$ matrices for the policy AGE, respectively

for Lombardia and Veneto, in the two panels of the Appendix Figure A–3. The matrices for all the other policies are reported in the Online Appendix. In all cases the time varying R_t matrices associated with the $R_{0,eq}$ matrices evolve according to the law of motion determined by the estimates of the behavioural response to mortality discussed in Section 4 and 6.4.2.

As expected, for each policy the $R_{0,eq}$ parameters grow with a combination of age, activity and riskiness of the sector (in case of activity). Most interactions (in particular those involving active subjects) have a $R_{0,eq}$ greater than one but, taking into account the population weights, the mean $R_{0,eq}$ corresponding to each policy (last column of Table A–1) is smaller. Therefore, the corresponding R_t matrix will decrease below 1 already at rather low levels of observed mortality because of the behavioural response.

We also assume that, during the simulated Phase 3, schools will be open and the interaction between students in the same class, given the adoption of protection measures, will imply a a risk of contagion. Note that workers in the education sectors (teachers and assistants) are classified by Barbieri et al. (2020) as operating in a high-risk sector and are treated accordingly in our simulation model, as a function of their age.

7.2 Dystopian Trade-off

Our main results are described in Figure 10 and 11. In these figures the vertical axis measures fatalities per million inhabitants while the horizontal axis measures GDP losses (relative to the GDP implied by the policy ALL), and the depicted lines describe, for the two regions and for four different scenarios, the frontier of the policies that are efficient, i.e. those yielding combinations of fatalities and GDP losses that are located on the lowest south-west convex envelope of the set of outcomes induced by all feasible policies.

An example of these efficient policies is provided in the Appendix, Table A–2.[17] The top part lists the efficient policies that are common to both regions, ordered from the one that maximizes fatalities and minimizes the GDP loss (ALL) to the one associated with the opposite effects (LOCK). The general pattern is clear: starting from policy ALL, in order to move down along the efficient contour it is necessary to progressively inactivate (i.e. allow only the minimum 60% of the labor force to be active) workers in the high-risk sector, beginning with those belonging to a higher age bracket, until LOCK is reached in which case all age brackets and sectors are inactivated. Some policies slightly deviate from this pattern, like for example AGE_SEC$_{12}$ and AGE_SEC$_{13}$, because labor force participation rates are not the same in all age brackets. The next two panels in the table describe policies that are efficient only in Lombardia (2) or Veneto (3), respectively.

[17] This example refers to the left panel of Figure 10, i.e. to the case of $\beta(m) = 0.8$ with behavioural response.

Figure 10: The efficient frontier in the two regions with $\beta(m) = 0.8$

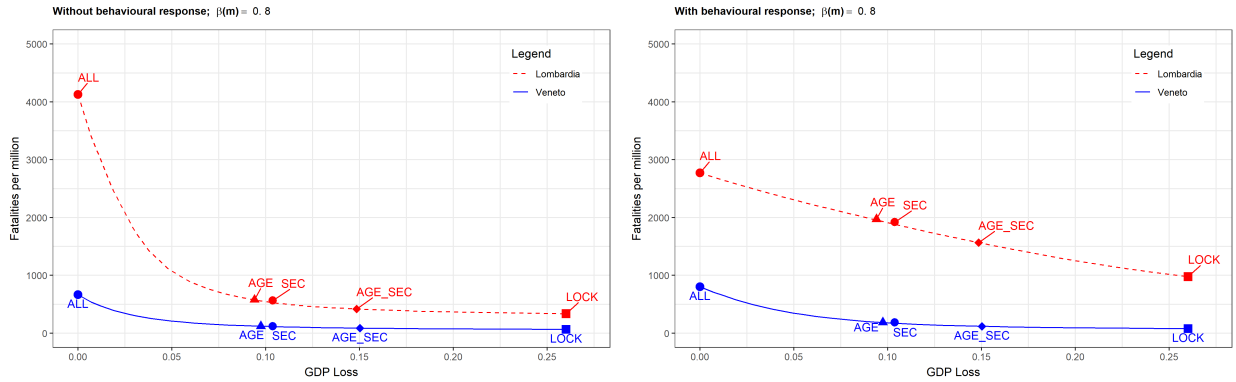

Note: In each panel, the two curves report the efficient frontiers for outcomes occurring between September 1, 2020, and August 31, 2021. Each point shows the GDP loss and the number of fatalities per million individuals associated to the policies that are efficient (as defined in the text). The representative policies are displayed in the same way. GDP losses are defined as relative to the GDP implied by the policy ALL.

The left panel of Figure 10 considers an hypothetical scenario in which $\beta(m) = 0.8$[18] and there is no behavioural response of the population to the number of fatalities. In this Scenario, the Policy ALL, that sends back to work all the active population, avoids any GDP loss but causes the maximum number of yearly fatalities in both regions, with Lombardia facing more than four times as many death per million inhabitants as Veneto (≈ 4000 versus ≈ 1000) over the year starting from September 1, 2020.

In Lombardia, however, there exists a number of efficient mixed strategies based on the age and sector criteria, that would reduce dramatically the total number of fatalities with relatively minor GDP losses until the threshold of approximately a 10 percent loss is encountered. Mixed policies that cause a loss of this size are associated to about 500 fatalities per million inhabitant in this region. Trying to reduce fatalities beyond this level causes a huge increase in GDP losses without saving many lives. Imposing a Lockdown for a full year after September 1 (LOCK) would cause a probably unsustainable GDP loss of almost 25 per cent. Given the more favourable situation in Veneto, due to the lower population density and to the remaining more effective hospital management policies, the kink observed for Lombardia is less pronounced in this region and occurs at a GDP loss around 5%.

An interestingly different pattern emerges in the right panel of Figure 10, where we allow individuals to respond to news about fatalities, based on the estimates in Table 2 of Section 4. In this scenario, for Lombardia we do not observe a kink at a GDP loss of 10% because when fatalities grow at a sufficiently high level, individuals begin to react by reducing mobility and thus infections. This behavioural response counterbalances the effect on fatalities deriving

[18]Remember that this parameters may be interpreted in two ways. One is that individuals are 20% more careful than normal in maintaining social distancing. The second is that aggressiveness of the virus declines by 20% for meteorological or other reasons.

from activating workers with the intent to decrease GDP losses below 10%. In other words, when the behavioural response kicks in, increasing the level of activity with workers of higher ages in more risky sector becomes possible with a lower cost in terms of fatalities.

In the case of Veneto, the low level of fatalities does not induce a strong behavioural response, and therefore the solid lines in the two panels are almost identical. Mixed policies pushing the GDP loss below 5% would increase fatalities but at levels that would not be sufficiently high to trigger the behavioural response.

The choice of which one of the specific efficient policies should be adopted depends of course on the weight society gives to fatalities versus GDP losses in the aggregate welfare function. However, the combination of the evidence in the two panels of Figure 10 suggests that even in the absence of a behavioural response to fatalities, there exists a wide set of policies differentiated by age and riskiness of sectors that would allow to reduce significantly GDP losses without a dramatic increase in fatalities. The existence of a behavioural response of the size we have estimated would help in reaching this goal and would become effective when most needed, i.e. at relatively high levels of fatalities as in Lombardia. Of course, this more desirable scenario hinges on the expectation that the behavioural response that we have estimated in Section 4 for the first three months of the pandemic persists in the long run, even when the population will have get used to the virus. If at that point habit formation will induce a weaker response to fatalities, the scenario of the left panel will be the most likely one.

Figure 11: The efficient frontier in the two regions with $\beta(m) = 1$

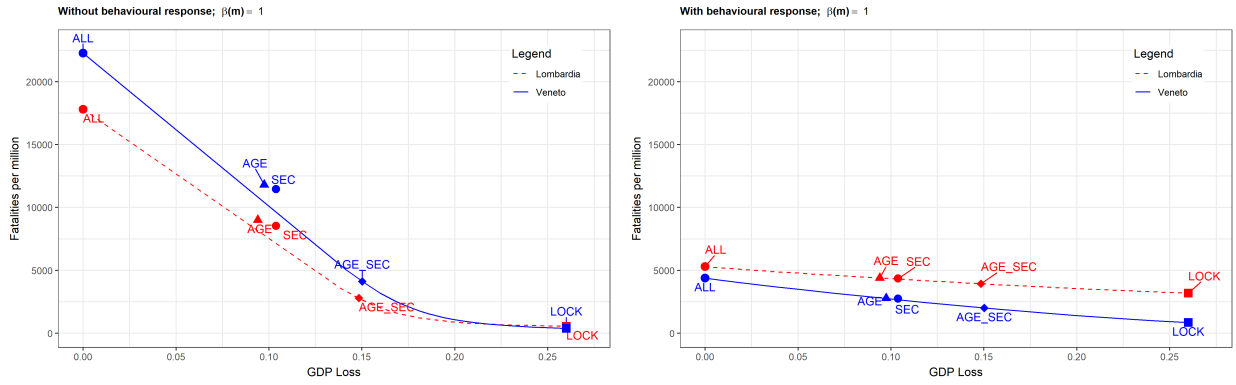

Note: In each panel, the two curves report the efficient frontiers for outcomes occurring between September 1, 2020, and August 31, 2021. Each point shows the GDP loss and the number of fatalities per million individuals associated to the policies that are efficient (as defined in the text). The representative policies are displayed in the same way. GDP losses are defined as relative to the GDP implied by the policy ALL.

Figure 11 replicates the same analysis for the case in which $\beta(m) = 1$. This parameter implies a low level of attention of the population in implementing social distancing or a high

level of aggressiveness of the virus. In this case, the scenario described by the left panel, without a behavioral response, is considerably more dramatic. Here we see that the kink is at a higher level of GDP loss with respect to the case in which $\beta(m) = 0.8$ (15% instead of 10%). Trying to reduce GDP losses below this level would lead in both regions to a huge increase in fatalities on a yearly basis (about 20500 in Lombardia and about 17500 in Veneto, per million inhabitants). At this level of the parameter $\beta(m)$ the existence of a behavioural response to fatalities at least as strong as the one we have estimated is crucial to allow for a substantial reduction of GDP losses that is not too costly in terms of lices. This is shown in the right Panel of Figure 11, where the kink disappears because the behavioural response operates in both regions. If the ALL policy were to be adopted with $\beta(m) = 1$ and in presence of a behavioural response, yearly fatalities would not go above the level of 5000 per million inhabitants.

As for the relative position of the efficient frontiers of the two regions with respect to fatalities for any level of GDP loss, Lombardia appears to have a relatively worse trade-off in all scenarios. One reason for this difference, as already mentioned, is the higher density of the population in this region. In addition, although the management of hospital flows has become more similar between the two regions, at least during the period for which we have data (see Section 5.2 and Figure 4), differences remain that make the public health system in Lombardia more fragile with respect to significant waves of infections. And this appears to be true even if the ICU capacity has been expanded in this region during the pandemic.

Figure 12 plots the daily fatalities predicted by the model for Lombardia allowing the prediction to differ, during the simulation year, according to the five representative policies that we consider. The left panels cover the entire period from January 1, 2020 to August 31, 2021. The right panels zoom into the year of simulation starting on September 1, 2020. The top panels are for the scenario in which $\beta(m) = 0.8$ and the population responds to fatalities. In this case, given the lower $\beta(m)$, Lombardia is unlikely to face a new wave of infection as dramatic as the one experienced in March, 2020, even if policy ALL were to be adopted and everybody went back to work. The line for the representative mixed policy AGE_SEC clearly indicates that the differentiation of containment by age and sector risk offers the possibility to effectively limit fatalities, without any need to lock down the entire economy.

The bottom panels assume $\beta(m) = 1$, while still allowing for the estimated behavioural response of the population to fatalities. In this case Lombardia will face a much worse second wave of infection during the winter of 2020-21, particularly if policy ALL is adopted. An interesting feature of this scenario, in line with the qualitative predictions of Cochrane (2020), is the oscillatory pattern of daily fatalities during the simulation year that we observe inde-

Figure 12: Daily fatalities under the different policies in Lombardia

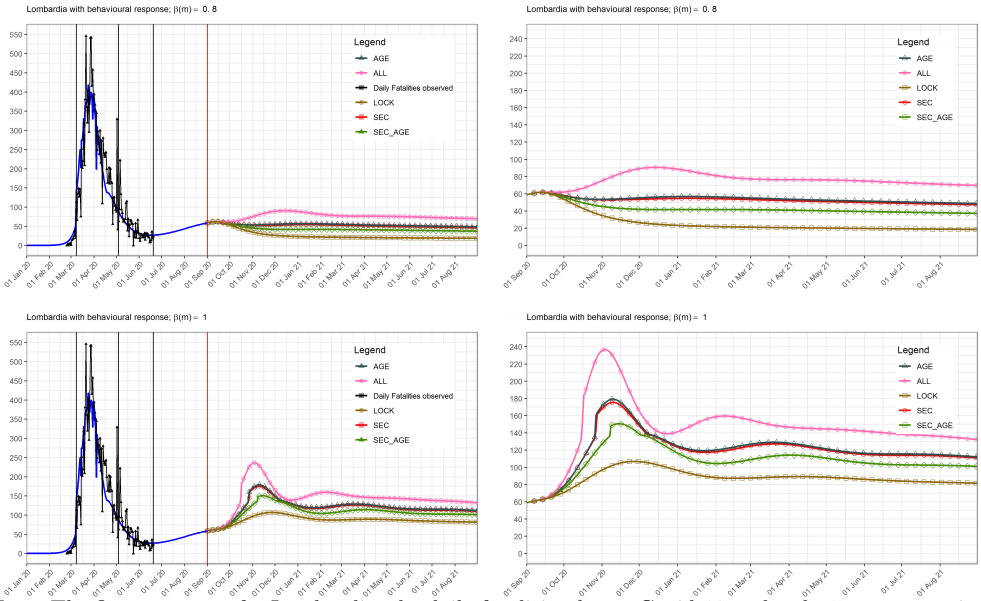

Note: The figure reports, for Lombardia, the daily fatalities due to Covid-19 under the 5 representative policies that we consider, for the scenario with behavioural response and $\beta(m) = 0.8$. The left panels cover the entire period from January 1, 2020 to August 31, 2021. The right panels zoom into the year of simulation starting on September 1 in order to better highlight the differences between the fatalities associated to each policy.

pendently of the adopted policy. These oscillations are the result of the behavioural response to fatalities in the population that is strong when fatalities are high, thereby contributing to contain the height of the wave, and weak when fatalities are low, contributing to facilitate the conditions for a subsequent wave.

In all these scenarios, the level of fatalities would be much higher in the absence of a behavioural response and the correspondent figures are in the Online Appendix. Figure 13 replicates the analysis of predicted daily fatalities for Veneto with qualitatively similar findings, starting from a much lower level of fatalities for the reasons illustrated in previous sections.

Tables 8 displays some summary statistics of the effects of the representative policies in Lombardia and Veneto. Here we want to highlight two interesting facts. First, in both regions herd immunity is unlikely to help in winning the battle against the virus. Even if everybody went back to work during the simulation year (Policy ALL), thus increasing the probability of infection, herd immunity would not grow to sufficiently high levels. Second, while the mean R_t over the simulation year is very similar for all the five emblematic policies and slightly smaller than 1 in all cases, what determines the different outcomes is the variability of R_t over time. For example, the high number of fatalities associated with policy ALL in Lombardia is a result of the fact that the maximum level of R_t is above 1 in this case. The

Figure 13: Daily fatalities under different policies in Veneto.

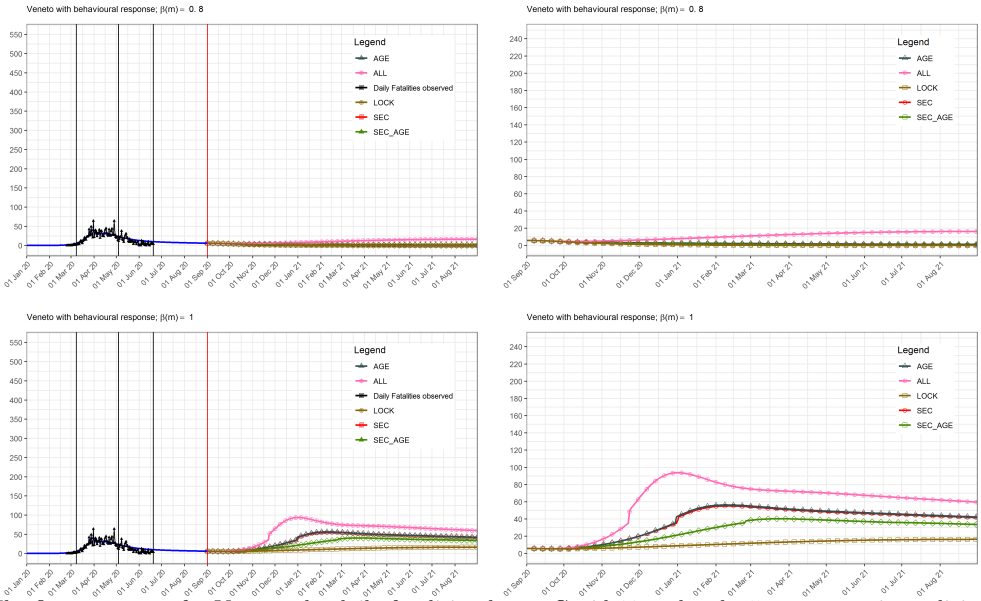

The figure reports, for Veneto, the daily fatalities due to Covid-19 under the 5 representative policies that we consider, for the scenario with behavioural response and $\beta(m) = 0.8$. The left panels cover the entire period from January 1, 2020 to August 31, 2021. The right panels zoom into the year of simulation starting on September 1 in order to better highlight the differences between the fatalities associated to each policy.

Online Appendix shows figures that display the evolution of R_t in the simulation year for the different policies in the two regions.

8 Conclusions

Compared to existing work in the now vast field of economics of a pandemic, this paper has several important distinctive features.

Quantitative Realism in Modeling. First of all, we have tried to make the model directly empirically relevant, aiming to provide precise (as much as possible) estimates and predictions of future developments. We are not interested here in providing qualitative regularities that can organize our thinking about the phenomenon: we want to provide a tool that measures consequences in terms of the most important outcomes (such as number of fatalities, loss of GDP, development of herd immunity in the population), and thus offers precise estimates of the tradeoffs between the values of these variables that follows specific, implementable, realistic policies. We want to provide a tool for the decision makers and the informed public opinion.

To achieve this objective of quantitative realism, we build, relying on Favero (2020), a model extending the classical $SEIR$ (which is the relevant epidemiological model in the case

Table 8: Lombardia and Veneto: main outcomes with behavioural response and $\beta(m) = 0.8$

	Policies				
	LOCK	SEC	AGE	SEC_AGE	ALL
Lombardia					
Total fatalities	9770	19209	19710	15678	27699
GDP loss	0.26	0.104	0.094	0.148	0
Final herd immunity	0.042	0.057	0.058	0.052	0.071
Average R_t	0.97 (0.88 - 0.98)	0.96 (0.95 - 0.97)	0.96 (0.95 - 0.97)	0.97 (0.93 - 0.98)	0.95 (0.92 - 1.02)
Veneto					
Total fatalities	389	896	920	579	3943
GDP loss	0.26	0.104	0.097	0.150	0
Final herd immunity	0.011	0.013	0.013	0.011	0.026
Average R_t	0.84 (0.83 - 0.85)	0.92 (0.90 - 0.92)	0.92 (0.91 - 0.93)	0.89 (0.88 - 0.90)	0.95 (0.92 - 0.98)

Note: The table reports the main outcomes of the five policies in Lombardia and Veneto, for the scenario with behavioural response and $\beta(m) = 0.8$, measured over the year between September 1, 2020 and August 31, 2021. Final herd immunity is calculated at the end of the simulation period taking into account the total exposed from January 1, 2020. The numbers in parentheses indicate the minimum and maximum Average R_t during the simulation period (they do not define a confidence interval).

the Covid-19 epidemic, as opposed for instance to SIR models) taking into account two broad orders of factors. The first is the constraints of hospital and health structures. This constraint is a crucial specific characteristic of the current epidemic, and explains many of the puzzling phenomena that have emerged (one instance is the difference of the spread of the epidemic in the two regions of Lombardia and Veneto). The second is the specific dynamic of the epidemics across different types of individuals and clinical conditions. This in turn allows us to take into due account the differences in fundamental biological parameters across ages. Only because we do this in a realistic way we can then calibrate the crucial parameters and provide an accurate estimate of policies differentiating the intervention depending on the age of the individuals.

Role of Hospitals and Health Structures. A crucial characteristic feature of the current epidemic has been its potential to overrun hospitals and health structures, introducing a significant non linearity in the number of fatalities as function of the number of infected. We have used as a proxy for the measure of stress on hospitals the fraction of use of ICU's. While we do not think that ICU have a dominant role in the ability of hospitals to save lives, the measure has proved to be in our data analysis an effective indicator of the performance of hospitals in care provision. This feature, together with the more obvious effect of population density, plays a crucial role in explaining the difference between the developments in Lombardia and Veneto, and is likely the most important explanation of other specific instances of the epidemic, such as, for example, its recent evolution in New York

City.

Identification of Efficient Policies. In line with our main aim, we have not tried to derive estimation of policies on the basis of a welfare function or the utility of a representative agent in a competitive economy with a public sector. Our main conclusions, when we evaluate policies, have been formulated as two main groups of findings. First, we want to identify the policies that are efficient, that is policies for which there is no other feasible policy that induces a better final outcome in all relevant outcomes. We think that public opinion and informed discussion should choose among these, and offer the analysis necessary to avoid policy mistakes. Second, we allow the comparison between any two of these policies to be reduced to a comparison between estimated specific values of the relevant outcomes. When the public is considering the shift from a policy to another, we are offering here an estimate of the costs and benefits of the two policies. We have no illusion that the numbers we offer are the true numbers: we are however convinced that having some estimate reasonably close to the truth is better that having only qualitative, sometimes obvious, statements. Navier-Stokes equation provides an approximation, just like we do, but planes fly on the basis of the approximation. Here the quantitative realism is essential: what matters is the size of the effect, not just its direction.

The results presented in Section 7 illustrate one of the main tools we offer to the public debate. The figures present the values of possibly the two most important variables (total number of fatalities and GDP loss over one year period) that our model associates to a menu of policy choices determining the number and groups of workers that are allowed back to work. In line with our efficiency criterion, we only provide the values associated with the policies that are not dominated by other feasible ones. The results are presented for two regions, that are emblematic of two very different evolutions of the current epidemic in Italy, Lombardia and Veneto. As expected, the precise trade-offs depend on the estimated underlying parameters, that are very different as anyone acquainted with the current debate in Italy knows. In spite of this, precise conclusions common to both cases can be drawn, which are therefore robust to the parameter specification.

Behavioral Adjustments. We have also provided an estimate, based on real data, of the effect of behavioral adjustments of individuals to the risk of infection. The estimation strategy is guided by a simple but effective model of how individuals balance the utility from mobility with the risk of getting infected, and how this response adjusts to the estimate of the number of infectious based on the current number of fatalities. The size of the effect of this adjustment is striking. Its magnitude, particularly in the early days of the epidemics, is comparable to the effects of the administrative measures taken in Italy in the months of March and April, which were severe. The Pareto curve, which is our measure of the trade-off

between fatalities and loss of GDP becomes almost flat as a consequence of these individual adjustments. The response is highly non linear: an additional increase in the risk (measured in our model by the number of fatalities) results in a flatter and flatter response of the mobility measures. We should also take into account that this estimate of the effect relies on the assumption that the size of the response will be in the future similar to what we have observed in the past; this assumption may be problematic.

Extensions. We have not explicitly considered, in this version of the paper, policies that are different according to regions (or macro regions, such as North and South). This extension is feasible, indeed easy within our framework, since it requires a calibration of the key parameters, as well as the number of Infectious in the initial period. Also, we have not modelled the impact of policies on the capital side of the production function and we have not considered fiscal policy interventions and their consequences to workers, firms and the sustainability of public debt. We plan to extend the simple macroeconomic structure adopted here to address all these issues in future work.

Costs and benefits of alternative policies that are widely discussed have not been considered explicitly, but can be easily adjusted within the current framework. Here we consider some examples. Increasing the number of IC units and training the personnel necessary to manage them has a financial cost, and a benefit in terms of fatalities. These unitary costs can be estimated, and the effect of the policy estimated. Testing, of all types, has clear costs, and benefits that can be formulated as reduction of the corresponding entries of the basic reproduction matrix. Testing of workers can substantially reduce contagion within a risk sector (low and high); and it can reduce the risk across risk classes (for instance affecting the contagion in mass transportation). Similarly, measures to reduce the spread during traveling affect the Tr parameter. Pharmacological remedies change the basic "biological" parameters, such as the p^{sev}, p^{ic} and p^{fat}. In summary, the purpose of the paper is to provide a method that is rich enough but tractable to quantify the benefits of alternative policies.

9 Appendix

Figure A–1: Basic Reproduction Matrices before Lockdown

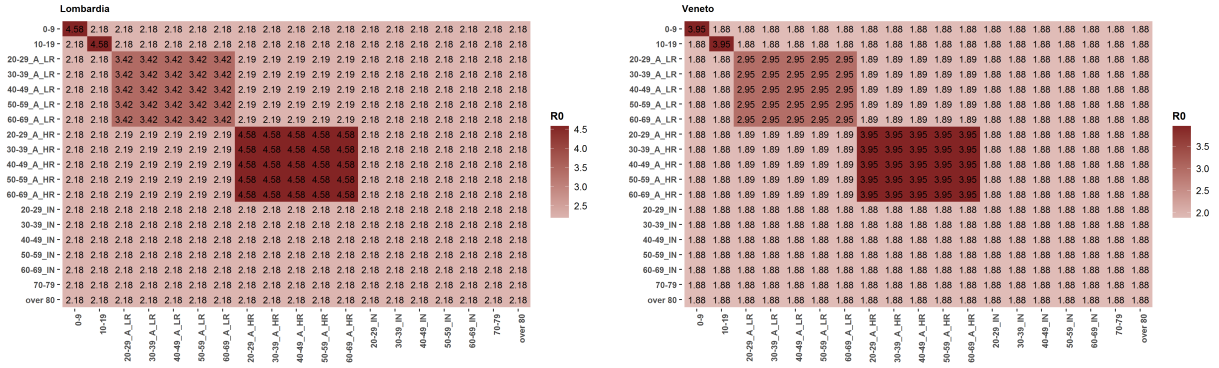

Note: Each cell in the table reports the R_0 for the interaction between an infectious subject of the category of the corresponding row and exposed subjects in the category of the corresponding column.

Figure A–2: Equivalent Basic Reproduction Matrices during Lockdown

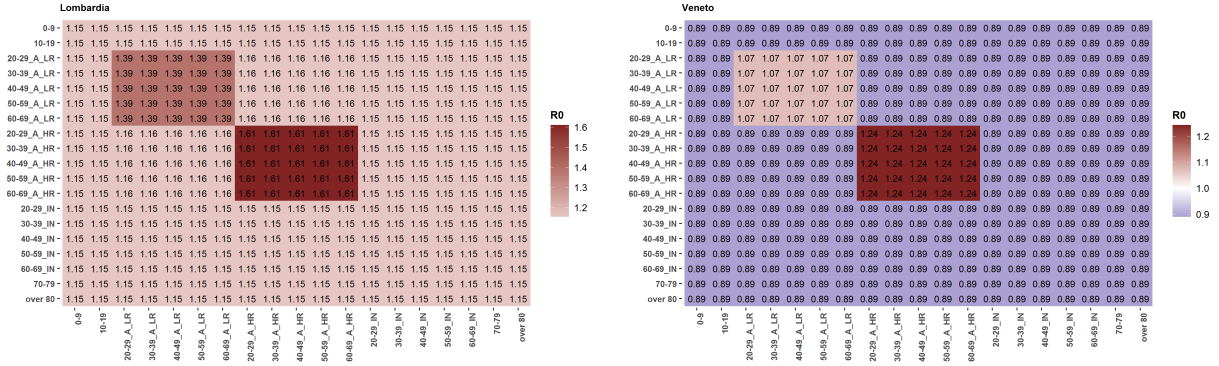

Note: Each cell in the table reports the R_0, eq for the interaction between an infectious subject of the category of the corresponding row and exposed subjects in the category of the corresponding column.

Figure A–3: Equivalent Basic Reproduction Matrices post-Lockdown for Policy AGE

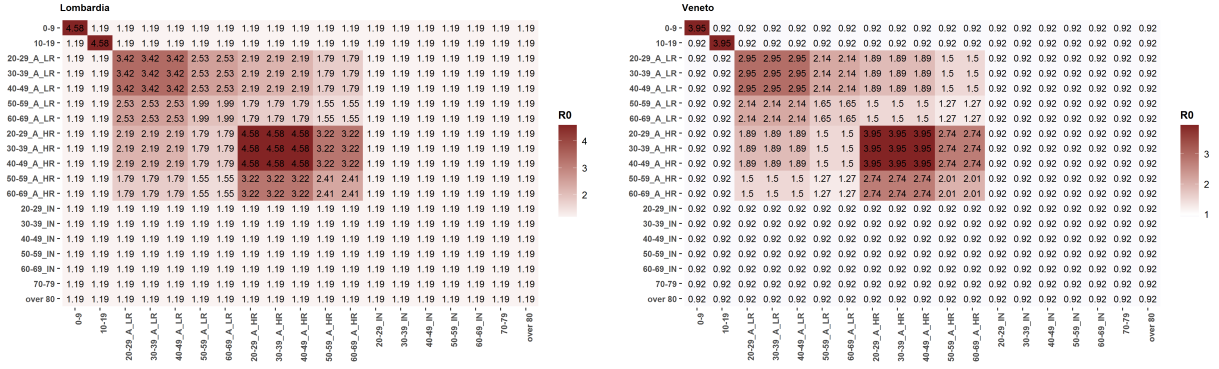

Note: Each cell in the table reports the R_0, eq with $\beta(m) = 1$ for the interaction between an infectious subject of the category of the corresponding row and exposed subjects in the category of the corresponding column.

Table A–1: Relevant $R_{0,eq}$ parameters for the different policies with $\beta(m) = 1$

	1	2	3	4	5	6	7	8	9	10	11	mean
Lombardia												
$p =$ LOCK	1.19	4.58	2.41	2.41	1.55	1.55	2.41	1.55	1.99	1.99	1.99	1.36
$p =$ SEC	1.19	4.58	2.41	2.41	1.79	1.79	2.41	1.79	3.42	3.42	3.42	1.48
$p =$ AGE	1.19	4.58	4.58	3.22	2.19	1.79	2.41	1.55	3.42	2.53	1.99	1.49
$p =$ AGE_SEC	1.19	4.58	*	**	***	****	2.41	1.55	3.42	2.53	1.99	1.44
$p =$ ALL	1.19	4.58	4.58	4.58	2.19	2.19	4.58	2.19	3.42	3.42	3.42	1.57
Veneto												
$p =$ LOCK	0.92	3.95	2.01	2.01	1.27	1.27	2.01	1.27	1.65	1.65	1.65	1.07
$p =$ SEC	0.92	3.95	2.01	2.01	1.5	1.5	2.01	1.5	2.95	2.95	2.95	1.17
$p =$ AGE	0.92	3.95	3.95	2.74	1.89	1.5	2.01	1.27	2.95	2.14	1.65	1.18
$p =$ AGE_SEC	0.92	3.95	#	##	###	####	2.01	1.27	2.95	2.14	1.65	1.14
$p =$ ALL	0.92	3.95	3.95	3.95	1.89	1.89	3.95	1.89	2.95	2.95	2.95	1.26

Note: For each policy indicated in a row and respectively for the two regions, the columns of this table report the $R_{0,eq}$ corresponding to the following interactions: 1) any interaction involving subjects at home; 2) students with students in the same class; 3) young active high-risk with young active high-risk; 4) young active high-risk with old active high-risk; 5) young active high-risk with young active low-risk; 6) young active high-risk with old active low-risk; 7) old active high-risk with old active high-risk; 8) old active high-risk with old active low-risk; 9) young active low-risk with young active low-risk; 10) young active low-risk with old active low-risk; 11) old active low-risk with old active low-risk. The last column reports, for each policy, the average R_0 in the population, obtained as an average of the R_0 for each type of interaction weighted by the size of the population involved. The table for the case in which $\beta(m) = 0.8$ can be easily obtained multiplying each number by 0.8.
For Lombardia:
** Given the structure of the policy there are 2 different values for this class: 3.22 for 20-29 to 50-69 and 2.41 for 30-49 to 50-69.
*** Given the structure of the policy there are 2 different values for this class: 2.19 for 20-29 to 20-49 and 1.79 for 30-49 to 20-49.
**** Given the structure of the policy there are 2 different values for this class: 1.79 for 20-29 to 50-69 and 1.55 for 30-49 to 50-69. For Veneto:
# Given the structure of the policy there are 3 different values for this class: 3.95 for 20-29 to 20-29, 2.74 for 30-49 to 20-29 and vice versa, and 2.01 for 30-49 to 30-49.
Given the structure of the policy there are 2 different values for this class: 2.74 for 20-29 to 50-69 and 2.01 for 30-49 to 50-69.
Given the structure of the policy there are 2 different values for this class: 1.89 for 20-29 to 20-49 and 1.5 for 30-49 to 20-49.
Given the structure of the policy there are 2 different values for this class: 1.5 for 20-29 to 50-69 and 1.27 for 30-49 to 50-69.

Table A–2: Worker activation vector of the efficient policies in Lombardia and Veneto with behavioural response and $\beta(m) = 0.8$

	Low-Risk sector Age brackets					High-Risk sector Age brackets				
Policy	20-29	30-39	40-49	50-59	60-65	20-29	30-39	40-49	50-59	60-65
Efficient AGE_SEC policies common to both regions										
$p =$ ALL	1	1	1	1	1	1	1	1	1	1
$p = AGE\_SEC_1$	1	1	1	1	1	1	1	1	1	0.6
$p = AGE\_SEC_2$	1	1	1	1	1	0.6	1	1	1	0.6
$p = AGE\_SEC_3$	1	1	1	1	1	1	1	1	0.6	1
$p = AGE\_SEC_4$	1	1	1	1	1	1	1	1	0.6	0.6
$p = AGE\_SEC_5$	1	1	1	1	0.6	1	1	1	0.6	0.6
$p = AGE\_SEC_6$	1	1	1	1	0.6	0.6	1	1	0.6	0.6
$p = AGE\_SEC_7$	1	1	1	1	0.6	1	0.6	1	0.6	0.6
$p = AGE\_SEC_8$	0.6	1	1	1	0.6	1	0.6	1	0.6	0.6
$p = AGE\_SEC_9$	0.6	1	1	1	0.6	1	1	0.6	0.6	0.6
$p = AGE\_SEC_{10}$	1	1	1	0.6	1	1	1	0.6	0.6	0.6
$p = AGE\_SEC_{11}$	1	1	1	0.6	1	0.6	0.6	0.6	0.6	0.6
$p = AGE\_SEC_{12}$	1	1	1	0.6	0.6	0.6	1	0.6	0.6	0.6
$p = AGE\_SEC_{13}$	0.6	1	1	0.6	0.6	0.6	1	0.6	0.6	0.6
$p = AGE\_SEC_{14}$	0.6	1	1	0.6	0.6	1	0.6	0.6	0.6	0.6
$p = AGE\_SEC_{15}$	1	0.6	1	0.6	0.6	1	0.6	0.6	0.6	0.6
$p = AGE\_SEC_{16}$	1	0.6	1	0.6	0.6	0.6	0.6	0.6	0.6	0.6
$p = AGE\_SEC_{17}$	1	1	0.6	0.6	0.6	1	0.6	0.6	0.6	0.6
$p = AGE\_SEC_{18}$	1	1	0.6	0.6	0.6	0.6	0.6	0.6	0.6	0.6
$p = AGE\_SEC_{19}$	0.6	1	0.6	0.6	0.6	0.6	0.6	0.6	0.6	0.6
$p = AGE\_SEC_{20}$	1	0.6	0.6	0.6	0.6	0.6	0.6	0.6	0.6	0.6
$p =$ LOCK	0.6	0.6	0.6	0.6	0.6	0.6	0.6	0.6	0.6	0.6
Efficient AGE_SEC policies for Veneto only										
$p = AGE\_SEC$	1	1	1	0.6	0.6	1	0.6	0.6	0.6	0.6
$p = AGE\_SEC_{21}$	1	1	1	1	1	0.6	1	1	1	1
$p = AGE\_SEC_{22}$	1	1	1	1	1	1	0.6	1	1	0.6
$p = AGE\_SEC_{23}$	1	1	1	1	0.6	0.6	1	1	0.6	1
$p = AGE\_SEC_{24}$	0.6	1	1	1	0.6	0.6	1	1	0.6	0.6
$p = AGE\_SEC_{25}$	0.6	1	1	1	0.6	1	1	0.6	0.6	1
$p = AGE\_SEC_{26}$	1	0.6	1	1	0.6	1	0.6	1	0.6	0.6
$p = AGE\_SEC_{27}$	1	1	1	0.6	1	1	0.6	1	0.6	0.6
$p = AGE\_SEC_{28}$	1	0.6	1	1	0.6	1	1	0.6	0.6	0.6
$p = AGE\_SEC_{29}$	1	1	1	0.6	0.6	1	0.6	1	0.6	0.6
$p = AGE\_SEC_{30}$	1	0.6	1	0.6	0.6	0.6	1	0.6	0.6	0.6
Other representative policies close to the efficient contour										
$p = SEC$	1	1	1	1	1	0.6	0.6	0.6	0.6	0.6
$p = AGE$	1	1	1	0.6	0.6	1	1	1	0.6	0.6

Note: This table reports the labor force activation vector for all the efficient and representative policies.

References

Acemoglu, D., Chernozhukov, V., Werning, I., Whinston, M.D., 2020. A multi-risk SIR model with optimally targeted lockdown. Technical Report. National Bureau of Economic Research.

Allen, L.J., 2017. A primer on stochastic epidemic models: Formulation, numerical simulation, and analysis. Infectious Disease Modelling 2, 128–142.

Alvarez, F.E., Argente, D., Lippi, F., 2020. A simple planning problem for covid-19 lockdown. Technical Report. National Bureau of Economic Research.

Atkeson, A., 2020. What Will Be the Economic Impact of COVID-19 in the US? Rough Estimates of Disease Scenarios. NBER WP 26867 .

Baqaee, D., Farhi, E., Mina, M.J., Stock, J.H., 2020. Reopening Scenarios. Technical Report. National Bureau of Economic Research.

Barbieri, T., Basso, G., Scicchitano, S., 2020. Italian workers at risk during the COVID-19 Epidemic. Mimeo .

Berger, D., Herkenhoff, K., Mongei, S., 2020. An seir infectious disease model with testing and conditional quarantine. BFI Working Paper NO. 2020-25 .

Boeri, T., Caiumi, A., Paccagnella, M., 2020. Mitigating the work-safety tradeoff. CEPR Covid Economics 2, 60–66.

Brotherhood, L., Kircher, P., Santos, C., Tertilt, M., 2020. An economic model of the Covid-19 epidemic: The importance of testing and age-specific policies. Technical Report. CESifo Working Paper.

Cochrane, J., 2020. A SIR model with behaviour. Technical Report. https://johnhcochrane.blogspot.com/2020/05/an-sir-model-with-behavior.html.

Durante, R., Gulino, G., Guiso, L., 2020. Asocial capital: Civic culture and social distancing during COVID-19. Technical Report. CEPR Discussion Paper No. DP14820.

Eichenbaum, M., Rebelo, S., Trabandt, M., 2020. The macroeconomics of epidemics'. london, centre for economic policy research. CEPR DP 14520 .

Fang, H., Wang, L., Yang, Y., 2020. Human mobility restrictions and the spread of the novel coronavirus (2019-ncov) in china,. NBER WP 26906 .

Farboodi, M., Jarosch, G., Shimer, R., 2020. Internal and external effects of social distancing in a pandemic. Technical Report. National Bureau of Economic Research.

Favero, C., 2020. Why is covid mortality in lombardy so high? evidence from the simulation of a seir-hc model. CEPR Covid Economics 4, 47–61.

Ferguson, N.M., Daniel, L., Gemma, N.G., Natsuk, o.I., Kylie, A., Marc, B., Sangeeta, B., Adhiratha, B., Zulma, C.c., Gina, C.D., Amy, D., Ilaria, D., Han, F.a., 2020. Impact of non-pharmaceutical interventions (npis) to reduce covid- 19 mortality and healthcare demand. Imperial College Covid-19 Response Team 2, 60–66.

Garg, S., 2020. Hospitalization rates and characteristics of patients hospitalized with laboratory-confirmed coronavirus disease 2019—covid-net, 14 states, march 1–30, 2020. MMWR. Morbidity and mortality weekly report 69.

Garibaldi, P., Moen, E.R., Pissarides, C.A., 2020. Modelling contacts and transitions in the sir epidemics model. Covid Economics Vetted and Real-Time Papers, CEPR .

Garriga, C., Manuelli, R., Sanghi, S., . Optimal Management of an Epidemic: An Application to COVID-19. A Progress Report. Technical Report. April 2020. mimeo.

Glover, A., Heathcote, J., Krueger, D., J., R.R., 2020. Health versus wealth: On the distributional effects of controlling a pandemic. CEPR DP 14606 .

Gollier, C., 2020. Cost-benefit analysis of age-specific deconfinement strategies. URL: https://drive. google. com/file/d/1Hs7VBjQC9OWn1a_vEyaTExf97uORKBId/view. Unpublished manuscript .

Greenstone, M., Nigam, V., 2020. Does social distancing matter? University of Chicago, BFIE WP 2020-26 .

Hall, R.E., Jones, I., Klenow, P.J., 2020. Trading off consumption and covid-19 deaths,. mimeo Stanford University .

Jones, C.J., Philippon, T., Venkateswaran, V., 2020. Optimal mitigation policies in a pandemic: Social distancing and working from home. Technical Report. National Bureau of Economic Research.

Kermack, W.O., McKendrick, A.G., 1927. A contribution to the mathematical theory of epidemics. Proceedings of the Royal Society of London. Series A, Containing Papers of a Mathematical and Physical Character 115 (772): 700– 721. 115, 700–721.

Kudlyak, M., Smith, L., Wilson, A., . Avoidance Behavior at the COVID19 Breakout in an SI3R Model. Technical Report. April 2020. mimeo.

Mossong, J., Hens, N., Jit, M., Beutels, P., Auranen, K., Mikolajczyk, R., Massari, M., Salmaso, S., Tomba, G.S., Wallinga, J., et al., 2008. Social contacts and mixing patterns relevant to the spread of infectious diseases. PLoS medicine 5.

Piguillem, F., Shi, L., 2020. The optimal covid-19 quarantine and testing policies. Mimeo, EIEF .

Rampini, A.A., 2020. Sequential lifting of covid-19 interventions with population heterogeneity. Technical Report. National Bureau of Economic Research.

Torrini, R., 2016. Labour, profit and housing rent shares in italian gdp: long-run trends and recent patterns. Banca d'Italia: Questioni di Economia e Finanza 318.